Bent-band theory of conductivity in heavily doped semiconductors at low temperatures

Masumi Takeshima
Electronics Research Laboratory, Matsushita Electronics Corporation, Takatsuki, Osaka 569, Japan
(Received 4 December 1986)

A theory is presented of the conductivity in heavily doped semiconductors at low temperatures on the basis of the bent-band model. With the use of the Green's-function formalism, the vertex part as well as the the free part of the two-particle Green's function is calculated, taking into account all the diagrams representing the electron-impurity interaction. An analytical expression convoluting the free part and the vertex part is obtained in a compact form represented by multiple integrations. The computation of the conductivity is carried out on n- and p-type Si and Ge and n-type GaAs at 0 K. Agreement between the theory and experiments is very good for Ge:As but is worse for Ge:Sb, Ge:Ga, Si:P, and Si:As. The cause of the good agreement for Ge:As is ascribed to the suitability of the impurity potential assumed for the calculation. However, the considerable agreement, which is found also for the other materials at doping levels down to that for the metal-insulator transition, suggests that the present theory may be more useful under another suitable choice of the impurity potential. The role of the vertex part is shown to be important especially at doping levels around that of the metal-insulator transition.

I. INTRODUCTION

The low-field conductivity in heavily doped semiconductors, especially that at low temperatures, is of academic interest because electrons interact strongly with many impurities simultaneously, as in the localization and delocalization problem. Various theories[1–7] have been developed so far in order to understand conduction in the presence of ionized impurities and to offer convenient methods of calculation. Although those theories have turned out to be useful[8,9] at high temperatures and/or low doping levels, they cannot explain[10] the conduction at high doping levels, especially at low temperatures, for the following reason. The above theories are exclusively based on a model in which electrons are scattered off the isolated impurities independently of all other earlier scatterings; the subsequent scatterings are also unaffected. Further, the electron-impurity scatterings are so strong that the second-order Born scattering considered in some of the above theories may be inadequate; higher-order scatterings may also have to be considered. Especially with regard to conduction around the metal-insulator transition, there seems to be no quantitatively satisfactory explanation based on numerical calculation.

This paper describes an attempt to obtain a quantitative understanding of the conduction at high doping levels and low temperatures, although the theory is useful also for high-temperature cases. Special interest is in the doping range around the metal-insulator transition. One approach to this problem is the use of the tight-binding approximation starting from a localized donor orbital.[11] This approach may be useful at low doping levels where the electronic states are not much extended, i.e., below the critical doping level of the metal-insulator transition. In contrast to the use of the tight-binding approximation, we adopt in this paper the bent-band model which has been used by Bonch-Bruevich[12] for analyzing the electronic states in heavily doped semiconductors. In this model, the spatial variation of the impurity potential is assumed to be gradual enough that the fluctuation in the energy of the states mirrors closely that in the potential energy. Using the bent-band model, the present author has discussed the electronic states in heavily doped semiconductors in the usual three-dimensional structures,[13] in quasi-two-dimensional structures,[14,15] and in quasi-one-dimensional structures.[16,17] In these analyses the diagram method of the Green's-function formalism has been used differently from Bonch-Bruevich's approach for the three-dimensional structures. We adopt that method also in this paper. Thus the present work is an extension of the previously developed method to the analysis of conduction in three-dimensional structures, and is a first step to further extension to lower-dimension cases.

In the discussion we will deal with the vertex part as well as the free part of the two-particle Green's function giving the conductivity. The two-particle Green's function is calculated by taking an ensemble average of the function over the impurity sites. It is shown that all the diagrams of the electron-impurity interaction appearing in the vertex part as well as in the free part can be summed; thus an analytical expression for the conductivity, convoluting the free part and the vertex part in one form, is obtained.

Actually there are some works[18–20] which have discussed the conductivity in three- and/or two-dimensional structures considering the vertex part. However, those works have been simplified by, for example, using a point-like impurity potential, the Born approximation, or a constant relaxation time. Although those calculations have turned out to be useful, especially for discussing weak localization, the models used are not appropriate for a quantitative understanding of the conduction in heavily

doped semiconductors at low temperatures. In particular, the importance of multisite scatterings has been pointed out[21] before. Use of an impurity potential with a reasonable model of the screening is crucial, together with an account of the multisite multiple Born scattering and of the wave-vector-dependent relaxation time, as is done in the present paper.

II. ANALYTICAL MODEL AND ONE-PARTICLE GREEN'S FUNCTION

In this section we present a model for the analysis of the impurity-scattering problem and give a brief description of the derivation of the one-particle Green's function because this function will be of special importance in the discussion of the conductivity. The derivation has been given by the present author on the basis of the diagram method and is given here in such a way as to facilitate the extension of the method to the calculation of the two-particle Green's function in the next section. First, we define our model by writing down the Hamiltonian

$$H = H_e + H_{e\text{-}i} + H_{e\text{-}e} \ . \tag{2.1}$$

Here H_e, $H_{e\text{-}i}$, and $H_{e\text{-}e}$ are the Hamiltonians for the band electrons, the electron-impurity interaction, and the electron-electron interaction, respectively. We assume H_e and $H_{e\text{-}i}+H_{e\text{-}e}$ to be the unperturbed Hamiltonian and the perturbation, respectively. The explicit forms of the Hamiltonians are

$$H_e = \sum_{l,\mathbf{k},\sigma} E_l(\mathbf{k}) a^\dagger_{l,\mathbf{k},\sigma} a_{l,\mathbf{k},\sigma} \ , \tag{2.2}$$

$$H_{e\text{-}i} = \frac{1}{V} \sum_{l',l,\mathbf{k},\mathbf{q},\sigma} \bar{\Gamma}_0(\mathbf{q}) a^\dagger_{l',\mathbf{k}+\mathbf{q},\sigma} a_{l,\mathbf{k},\sigma} \ , \tag{2.3}$$

$$H_{e\text{-}e} = \frac{1}{2V} \sum_{\substack{l_1,l_2,l_3,l_4 \\ \mathbf{k}',\mathbf{k},\mathbf{q},\sigma,\sigma'}} \bar{U}_0(\mathbf{q}) a^\dagger_{l_1,\mathbf{k}+\mathbf{q},\sigma} a^\dagger_{l_2,\mathbf{k}'-\mathbf{q},\sigma'} \times a_{l_3,\mathbf{k}',\sigma'} a_{l_4,\mathbf{k},\sigma} \ . \tag{2.4}$$

Here $a^\dagger_{l,k}$, $a_{l,k}$, and $E_l(\mathbf{k})$ are the creation operator, the annihilation operator, and the unperturbed subband energy, respectively, for the electron in subband l with wave vector $\mathbf{k}$ and spin σ. $\bar{\Gamma}_0(\mathbf{q})$ is the Fourier transform of the unscreened potential $\Gamma_0(\mathbf{r})$ due to all the impurities:

$$\Gamma_0(\mathbf{r}) = \sum_{n=1}^{N_i} U_{i0}(\mathbf{r}-\mathbf{R}_n) = \frac{1}{V} \sum_{\mathbf{q}} \bar{\Gamma}_0(\mathbf{q}) \exp(j\mathbf{q}\cdot\mathbf{r}) \ , \tag{2.5}$$

where $U_{i0}(\mathbf{r}-\mathbf{R}_n)$ is the unscreened potential due to the impurity at $\mathbf{r}=\mathbf{R}_n$. N_i is the total number of the impurities and V the crystal volume. $\bar{U}_0(\mathbf{q})$ is the Fourier transform of the interaction $U_0(\mathbf{r}_1-\mathbf{r}_2)$ between the electrons at $\mathbf{r}_1$ and $\mathbf{r}_2$, i.e.,

$$U_0(\mathbf{r}_1-\mathbf{r}_2) = \frac{e^2}{|\mathbf{r}_1-\mathbf{r}_2|} = \frac{1}{V} \sum_{\mathbf{q}} \bar{U}_0(\mathbf{q}) \exp[j\mathbf{q}\cdot(\mathbf{r}_1-\mathbf{r}_2)] \ , \tag{2.6}$$

where e is the electronic charge. Hereafter we consider ionized impurities of a single species. Then we have $U_{i0}(\mathbf{r}) = ZU_0(\mathbf{r})$, where Z is the negative of the valency of each impurity with respect to the host lattice. Defining $\bar{U}_{i0}(\mathbf{q})$ as the Fourier transform of $U_{i0}(\mathbf{r})$ similarly as in Eq. (2.5), we obtain

$$\bar{\Gamma}_0(\mathbf{q}) = \bar{U}_{i0}(\mathbf{q}) h(\mathbf{q}) \ , \tag{2.7}$$

$$h(\mathbf{q}) = \sum_{n=1}^{N_i} \exp(-j\mathbf{q}\cdot\mathbf{R}_n) \ , \tag{2.8}$$

$$\bar{U}_{i0}(\mathbf{q}) = Z\bar{U}_0(\mathbf{q}) = \frac{4\pi e^2 Z}{q^2} \ . \tag{2.9}$$

For generality we consider the case of arbitrary temperature including zero. Considering that we need the retarded Green's function finally, we must start with the temperature Green's function when the electron-electron interaction is considered; from that function the retarded Green's function can be found.[22] For the problem of the electron-impurity interaction, on the other hand, we can directly start with the retarded Green's function. In the analysis that follows, we neglect the effect of the intersubband scattering for the electron-impurity and the electron-electron interactions.

In the presence of the impurities, the one-particle retarded Green's function is expressed in terms of two wave vectors $\mathbf{k}$ and $\mathbf{k}'$, one energy parameter ω, and the position vectors of the randomly distributed impurities $\mathbf{R}_1, \mathbf{R}_2, \ldots, \mathbf{R}_{N_i}$ as $G^R(l\mathbf{k}, l\mathbf{k}';\omega;\mathbf{R}_1,\mathbf{R}_2,\ldots,\mathbf{R}_{N_i})$, whose dependence on the impurity sites comes from $h(\mathbf{q})$ of Eq. (2.7). For this Green's function we take an ensemble average[12,23] over the impurity sites, which is defined as

$$\langle G^R(l\mathbf{k}, l\mathbf{k}';\omega)\rangle = \frac{1}{V^{N_i}} \int d\mathbf{R}_1 d\mathbf{R}_2 \cdots d\mathbf{R}_{N_i} G^R(l\mathbf{k}, l\mathbf{k}';\omega;\mathbf{R}_1,\mathbf{R}_2,\ldots,\mathbf{R}_{N_i}) = G^R(l\mathbf{k},\omega)\Delta(\mathbf{k}-\mathbf{k}') \ . \tag{2.10}$$

Here $\Delta(\mathbf{q})$ is defined as $\Delta(\mathbf{q})=1$ if $\mathbf{q}=0$ and $\Delta(\mathbf{q})=0$ otherwise. The last step of Eq. (2.10) comes from the fact that the space uniformity, which is lost under random distribution of the impurities giving $\mathbf{k}\neq\mathbf{k}'$, is restored under the average distribution giving momentum conservation $\mathbf{k}=\mathbf{k}'$. $G^R(l\mathbf{k},\omega)$ is the retarded Green's function in the average impurity distribution, for which the rule of the diagram method is known.[23] Into $G^R(l\mathbf{k},\omega)$ the effect of the electron-electron Green's function can be incorporated by the standard diagram method. The discussion just above applies also to the temperature Green's function in the same way. Using the temperature Green's function obtained in this way, the dielectric screening of a bare potential can be obtained in terms of the polarization diagram. Based on this screening, we replace the unscreened potentials $\bar{\Gamma}_0(\mathbf{q})$, $\bar{U}_{i0}(\mathbf{q})$, and $\bar{U}_0(\mathbf{q})$ with the screened ones $\bar{\Gamma}(\mathbf{q})$, $\bar{U}_i(\mathbf{q})$, and $\bar{U}(\mathbf{q})$, respectively, in the following discussions.

Now we discuss the one-particle retarded Green's function $G^R(l\mathbf{k},l\mathbf{k}';\omega)$ (the position vectors of the impurities are omitted) considering only the electron-impurity interaction for which the screened potential is used. It can be shown[13] that we have

$$G^R(l\mathbf{k},l\mathbf{k}';\omega)=\frac{1}{V}\int d\mathbf{r}\exp[j(\mathbf{k}-\mathbf{k}')\cdot\mathbf{r}]\times\frac{1}{\omega+j0^+-E_l(\mathbf{k}+j\nabla_r)-\Gamma(\mathbf{r})}\ , \tag{2.11}$$

where $\nabla_r=\partial/\partial\mathbf{r}$; $\Gamma(\mathbf{r})$ is obtained from Eq. (2.5) by replacing the unscreened potentials $\Gamma_0(\mathbf{r})$ and $\bar{\Gamma}_0(\mathbf{q})$ with the screened ones $\Gamma(\mathbf{r})$ and $\bar{\Gamma}(\mathbf{q})$, respectively. Let us use the bent-band model where the spatial variation of the impurity potential is gradual enough. Thus we neglect the spatial derivatives of all orders of $\Gamma(\mathbf{r})$ in Eq. (2.11). Then we obtain

$$\begin{aligned}G^R(l\mathbf{k},l\mathbf{k}';\omega)&=\frac{1}{V}\int d\mathbf{r}\frac{1}{\omega+j0^+-E_l(\mathbf{k})-\Gamma(\mathbf{r})}\exp[j(\mathbf{k}-\mathbf{k}')\cdot\mathbf{r}]\\&=G_0^R(l\mathbf{k},\omega)\sum_{m=0}^{\infty}\frac{1}{V}\int d\mathbf{r}[G_0^R(l\mathbf{k},\omega)\Gamma(\mathbf{r})]^m\exp[-j(\mathbf{k}-\mathbf{k}')\cdot\mathbf{r}]\\&=G_0^R(l\mathbf{k},\omega)\sum_{m=0}^{\infty}\sum_{\mathbf{q}_1,\mathbf{q}_2,\cdots,\mathbf{q}_m}\Delta(\mathbf{q}_1+\mathbf{q}_2+\cdots+\mathbf{q}_m-\mathbf{k}_1+\mathbf{k}_2)\prod_{\alpha=1}^{m}[G_0^R(l\mathbf{k},\omega)\bar{\Gamma}(\mathbf{q}_\alpha)]\ ,\end{aligned} \tag{2.12}$$

where $G_0^R(l\mathbf{k},\omega)$ is the free-particle Green's function

$$G_0^R(l\mathbf{k},\omega)=\frac{1}{\omega+j0^+-E_l(\mathbf{k})}\ . \tag{2.13}$$

Now the ensemble average of $G^R(l\mathbf{k},l\mathbf{k}';\omega)$ over all the impurity sites is taken. From the last step of Eq. (2.12) and the relation $\bar{\Gamma}(\mathbf{q})=\bar{U}(\mathbf{q})h(\mathbf{q})$ corresponding to Eq. (2.7), we obtain[23] a diagram of the self-energy for $G^R(l\mathbf{k},\omega)$ as shown in Fig. 1 for the case of $n=4$. Such a diagram gives the self-energy

$$S(\mathbf{M}_n)=N_i^n[G_0^R(l\mathbf{k},\omega)]^{M_n-1}\prod_{\mu=1}^{n}H_{m_\mu}\ , \tag{2.14}$$

where we define $\mathbf{M}_n=(m_1,m_2,\ldots,m_n)$ by $\sum_{\mu=1}^{n}m_\mu=M_n$ and

$$H_m=\sum_{\mathbf{q}_1,\mathbf{q}_2,\cdots,\mathbf{q}_m}\Delta(\mathbf{q}_1+\mathbf{q}_2+\cdots+\mathbf{q}_m)\prod_{\alpha=1}^{m}\left[\frac{\bar{U}_i(\mathbf{q}_\alpha)}{V}\right]\ ; \tag{2.15}$$

m_α in Eq. (2.14) represents the number of interaction lines connected with the αth site. With the use of

$$U_i(\mathbf{r})=\frac{1}{V}\sum_{\mathbf{q}}\bar{U}_i(\mathbf{q})\exp(j\mathbf{q}\cdot\mathbf{r}) \tag{2.16}$$

we obtain

$$H_m=\frac{1}{V}\int d\mathbf{r}[U_i(\mathbf{r})]^m\ , \tag{2.17}$$

giving finally

$$S(\mathbf{M}_n)=\frac{n_i^n}{G_0^R(l\mathbf{k},\omega)}\int\mathcal{D}\mathbf{r}_n\prod_{\mu=1}^{n}(u_\mu)^{m_\mu}\ . \tag{2.18}$$

Here we define $\int\mathcal{D}\mathbf{r}_n=\int d\mathbf{r}_1\int d\mathbf{r}_2\cdots\int d\mathbf{r}_n$, $u_\mu=G_0^R(l\mathbf{k},\omega)U_i(\mathbf{r}_\mu)$, and the impurity concentration

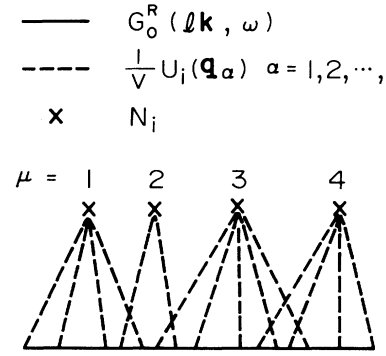

FIG. 1. Diagram representing the multisite multiple impurity scattering, which is obtained by taking an ensemble average over the impurity sites, for the case of $n=4$.

$n_i = N_i/V$.

Now we calculate the self-energy $\Sigma_i^R(l\mathbf{k},\omega)$ for the electron-impurity interaction alone, which is a sum of all the irreducible diagrams, as shown by examples in Fig. 2. For this purpose it is convenient to consider a sum of all the irreducible and reducible diagrams $\bar{P}$ which is expressed as

$$\bar{P} = \sum_{n=1}^{\infty} \frac{1}{n!} \sum_{M_n=n}^{\infty} \sum_{\mathbf{M}_n}' P(\mathbf{M}_n;M_n) S(\mathbf{M}_n) , \tag{2.19}$$

where $\sum_{\mathbf{M}_n}'$ means a restricted summation over $\mathbf{M}_n = (m_1, m_2, \ldots, m_n)$ excluding $m_\mu = 0$ $(\mu = 1,2,\ldots,n)$, and we define

$$P(\mathbf{M}_k, M_n) = \frac{M_n!}{m_1! m_2! \cdots m_k!} \tag{2.20}$$

under $\sum_{\alpha=1}^{k} m_\alpha = M_n$ with $k \leq n$. Since $\bar{P}$ is related to $\Sigma_i^R(l\mathbf{k},\omega)$ by

$$\bar{P} = \Sigma_i^R(l\mathbf{k},\omega) + \Sigma_i^R(l\mathbf{k},\omega) G_0^R(l\mathbf{k},\omega) \bar{P} , \tag{2.21}$$

we obtain

$$\Sigma_i^R(l\mathbf{k},\omega) = \frac{\bar{P}}{1 + \bar{P} G_0^R(l\mathbf{k},\omega)} . \tag{2.22}$$

Now let us calculate $\bar{P}$, starting with the definition of

$$Q(k;M_n) = \sum_{\mathbf{M}_k}' P(\mathbf{M}_k;M_n) \int \mathcal{D}\mathbf{r}_n \prod_{\alpha=1}^{k} (u_\alpha)^{m_\alpha} , \tag{2.23}$$

$$R(k;M_n) = \sum_{\mathbf{M}_k} P(\mathbf{M}_k;M_n) \int \mathcal{D}\mathbf{r}_n \prod_{\alpha=1}^{k} (u_\alpha)^{m_\alpha} . \tag{2.24}$$

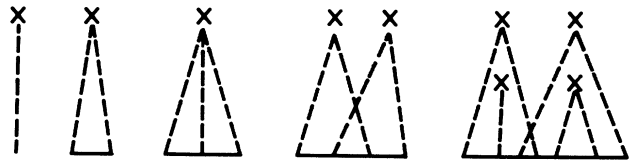

FIG. 2. Irreducible diagrams giving the self-energy for the impurity scattering.

The sum $\sum_{\mathbf{M}_k}$ in Eq. (2.24) is taken over $\mathbf{M}_k = (m_1, m_2, \ldots, m_n)$, where m_α can be zero as well as a positive integer under the condition that at least one of m_α's should not be zero so as to satisfy $m_1 + m_2 + \cdots + m_k = M_n$ $(\neq 0)$. As is shown in Appendix A, $Q(k;M_n)$ is related to $R(k;M_n)$ by the formula

$$Q(k;M_n) = \sum_{\alpha=0}^{k-1} (-1)^\alpha \binom{k}{\alpha} R(k-\alpha;M_n) . \tag{2.25}$$

Equation (2.24) can be given in a simple form:

$$R(k;M_n) = V^{n-k} \int \mathcal{D}\mathbf{r}_k (u_1 + u_2 + \cdots + u_k)^{M_n} . \tag{2.26}$$

Noting the relation $S(\mathbf{M}_n) = [n_i^n / G_0^R(l\mathbf{k},\omega)] Q(n;M_n)$ and using Eqs. (2.24), (2.25), and (2.26), Eq. (2.19) is rewritten as

$$\bar{P} = \frac{1}{G_0^R(l\mathbf{k},\omega)} \sum_{n=1}^{\infty} \frac{n_i^n}{n!} \sum_{M_n=1}^{\infty} \sum_{\alpha=0}^{n-1} (-1)^\alpha \binom{n}{\alpha} V^\alpha \int \mathcal{D}\mathbf{r}_{n-\alpha} (u_1 + u_2 + \cdots + u_{n-\alpha})^{M_n} . \tag{2.27}$$

It should be noted that the minimum value of M_n has been changed from n in Eq. (2.19) to 1 in Eq. (2.27) on account of Eq. (2.25) giving $Q(n;M_n) = 0$ under $1 \leq M_n < n$. With the use of the relation

$$\frac{1}{1 - \sum_\alpha u_\alpha} = \frac{1}{jG_0^R(l\mathbf{k},\omega)} \int_0^\infty ds \exp\left[j \left\{ \frac{1}{G_0^R(l\mathbf{k},\omega)} - \sum_\alpha U_i(\mathbf{r}_\alpha) \right\} s \right] , \tag{2.28}$$

Eq. (2.27) is rewritten, after performing all summations in Eq. (2.27), as

$$\bar{P} = \frac{1}{jG_0^R(l\mathbf{k},\omega)} \int_0^\infty ds \exp\left[\frac{js}{G_0^R(l\mathbf{k},\omega)} \right] \times \{\exp[n_i V h(s)] - 1\} , \tag{2.29}$$

where

$$H(s) = \frac{1}{V} \int d\mathbf{r} \{\exp[-jsU_i(\mathbf{r})] - 1\} . \tag{2.30}$$

Let us consider now the electron-electron interaction. This can be done simply by replacing $G_0^R(l\mathbf{k},\omega)$ in all the diagrams considered above with $G_1^R(l\mathbf{k},\omega)$, which is the retarded Green's function obtained by taking into account the electron-electron interaction alone. The function $G_1^R(l\mathbf{k},\omega)$ is given in the form

$$G_1^R(l\mathbf{k},\omega) = \frac{1}{\omega - E_l(\mathbf{k}) - \Sigma_e^R(l\mathbf{k},\omega)} , \tag{2.31}$$

where $\Sigma_e^R(l\mathbf{k},\omega)$ is the self-energy for the electron-electron interaction. As a result, the complete Green's function is obtained as:

$$G^R(l\mathbf{k},\omega)=\frac{1}{[G_1^R(l\mathbf{k},\omega)]^{-1}-\Sigma_i^R(l\mathbf{k},\omega)}$$
$$=\frac{1}{j}\int_0^\infty ds\,\exp\{js[\omega-E_l(\mathbf{k})-\Sigma_e^R(l\mathbf{k},\omega)]$$
$$+n_i Vh(s)\}\ . \tag{2.32}$$

This is a general expression for the complete Green's function representing the effect of the electron-impurity and the electron-electron interactions.

Although we can take into account all the diagrams for $\Sigma_e^R(l\mathbf{k},\omega)$, we consider here only the lowest-order diagram as shown in Fig. 3. We neglect also the exchange term, whose effect on the conductivity may be small, and take only the Coulomb term. For the diagram in Fig. 3, we use the complete Green's function $G^R(l\mathbf{k},\omega)$ including the effect of both the electron-impurity and the electron-electron interactions. Starting with the temperature Green's function, we obtain

$$\Sigma_e^R(l\mathbf{k},\omega)=-\frac{2\bar{U}(0)}{\pi V}\sum_{l,\mathbf{k}}\int d\omega\,\mathrm{Im}G^R(l\mathbf{k},\omega)\Theta(\omega)\ , \tag{2.33}$$

where $\Theta(\omega)$ is the Fermi-Dirac distribution function for energy measured from the Fermi level, i.e.,

$$\Theta(\omega)=\frac{1}{\exp\left[\dfrac{\omega}{T}\right]+1}\ ; \tag{2.34}$$

T is the thermal energy. The density of states $\rho(\omega)$ is given by

$$\rho(\omega)=-\frac{2}{\pi V}\sum_{l,\mathbf{k}}\mathrm{Im}G^R(l\mathbf{k},\omega)\ . \tag{2.35}$$

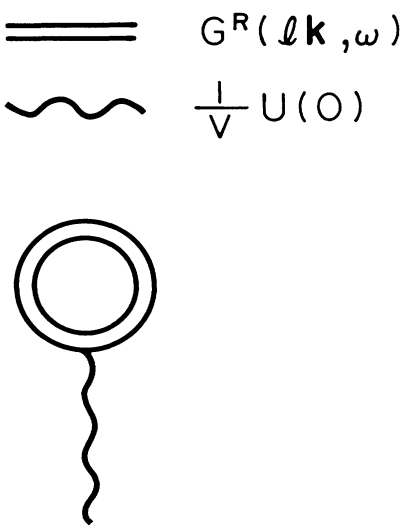

FIG. 3. Diagram representing the Coulomb term of the electron-electron interaction.

On the other hand, the electron concentration $|Z|n_i$ is given by

$$|Z|n_i=\int d\omega\,\rho(\omega)\Theta(\omega)\ . \tag{2.36}$$

As a result we obtain

$$\Sigma_e^R(l\mathbf{k},\omega)=|Z|n_i\bar{U}(0)\ . \tag{2.37}$$

III. CONDUCTIVITY AND TWO-PARTICLE GREEN'S FUNCTION

Again we start with the Green's function with two wave vectors of which the ensemble average over the impurity sites is not taken yet. In terms of the function, an expression for the dc conductivity tensor $\sigma_{\mu\nu}$ has been given by Bonch-Bruevich.[24] We put this into a more tractable form in Appendix B. For cubic symmetry we have $\sigma_{\mu\nu}=\Delta(\mu-\nu)\sigma$ and we obtain

$$\sigma=-\frac{2}{3\pi V}\frac{e^2\hbar^3}{(m^*)^2}\sum_{l,\mathbf{k}_1,\mathbf{k}_2}\int d\omega\frac{d}{d\omega}\Theta(\omega)$$
$$\times\mathrm{Im}G^R(l\mathbf{k}_1,l\mathbf{k}_2;\omega)$$
$$\times\mathrm{Im}G^R(l\mathbf{k}_2,l\mathbf{k}_1;\omega)\ , \tag{3.1}$$

where m^* is the effective mass. In practice we calculate σ by taking an ensemble average of the above product of the two-particle Green's function, i.e.,

$$\langle\mathrm{Im}G^R(l\mathbf{k}_1,l\mathbf{k}_2;\omega)\mathrm{Im}G^R(l\mathbf{k}_2,l\mathbf{k}_1;\omega)\rangle$$
$$=-\tfrac{1}{2}\mathrm{Re}[\langle G^R(l\mathbf{k}_1,l\mathbf{k}_2;\omega)G^R(l\mathbf{k}_2,l\mathbf{k}_1;\omega)\rangle$$
$$-\langle G^R(l\mathbf{k}_1,l\mathbf{k}_2;\omega)G^A(l\mathbf{k}_2,l\mathbf{k}_1;\omega)\rangle]\ , \tag{3.2}$$

where $G^A(l\mathbf{k}_2,l\mathbf{k}_1;\omega)$ is the advanced Green's function. Then the problem is reduced to the calculation of the averaged two-particle Green's function

$$K^{R,A}(l\mathbf{k}_1,l\mathbf{k}_2;\omega)=\langle G^R(l\mathbf{k}_1,l\mathbf{k}_2;\omega)G^{R,A}(l\mathbf{k}_2,l\mathbf{k}_1;\omega)\rangle\ , \tag{3.3}$$

where the affix R,A means selective choice of R or A according to the use of the retarded or advanced Green's function, respectively. The rule of the diagram sum for $K^{R,A}(l\mathbf{k}_1,l\mathbf{k}_2;\omega)$ is found by using Eq. (2.12) and is nearly the same as in the case of the one-particle Green's function. The method in the preceding section is of extended use here.

Figure 4 shows a diagram for $K^{R,A}(l\mathbf{k}_1,l\mathbf{k}_2;\omega)$ representing the electron-impurity interaction. Let us call as the A group the group of the sites through which the upper line (G^R) and the lower line ($G^{R,A}$) interact with each other through interaction lines. The groups of the sites giving interactions only in the upper line and only in the lower line are called the B group and the C group, respectively, as shown in the figure. Let the numbers of the sites for the A, B, and C group be a, b, and c; a, b, and c can be zero. As shown in Fig. 5, the two-particle Green's function $K^{R,A}$ is given as a sum of the free part and the

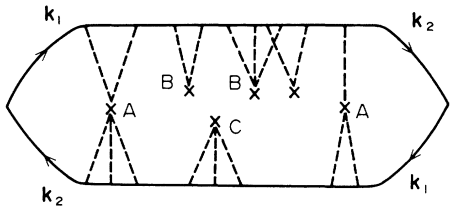

FIG. 4. Diagram representing the two-particle Green's function $K^R(l\mathbf{k}_1,l\mathbf{k}_2;\omega)$ for the electron-impurity interaction.

vertex part, which are represented by the case of $a=0$ and $a\geq 1$, respectively. The sum of q's for the interaction lines connected with a given site should be zero in all the groups. The sums of q's for all the interaction lines connected with the upper line and the lower line should be $\mathbf{k}_1-\mathbf{k}_2$ and $-(\mathbf{k}_1-\mathbf{k}_2)$, respectively. Correspondingly, in place of Eq. (2.15), there appears

$$H_m(\mathbf{p}_\mu)=\sum_{\mathbf{q}_1,\mathbf{q}_2,\cdots,\mathbf{q}_m}\Delta(\mathbf{q}_1+\mathbf{q}_2+\cdots+\mathbf{q}_m+\mathbf{p}_\mu)\times\prod_{\alpha=1}^{m}\left[\frac{\bar{U}_i(\mathbf{q}_\alpha)}{V}\right] \tag{3.4}$$

for those interaction lines of a given group which are connected with the μth site and with the upper or lower line. We have $\mathbf{p}_\mu=0$ for both the B and C group and $\mathbf{p}_\mu\neq 0$ for the A group. A sum $\sum_\mu \mathbf{p}_\mu$ for the upper line and the lower line should be equal to $\mathbf{k}_1-\mathbf{k}_2$ and $-(\mathbf{k}_1-\mathbf{k}_2)$, respectively.

Equation (3.4) is rewritten as

$$H_m(\mathbf{p}_\mu)=\frac{1}{V}\int d\mathbf{r}[U_i(\mathbf{r})]^m\exp(j\mathbf{p}_\mu\cdot\mathbf{r}) \tag{3.5}$$

as a more general form of Eq. (2.17). Corresponding to the relation between the one-particle Green's function and Eq. (2.14), the two-particle Green's function is related to $S(\mathbf{M},\mathbf{N})$, given by

$$S(\mathbf{M},\mathbf{N})=N_i^{a+b+c}[G_0^R(l\mathbf{k}_1,\omega)]^{M-1}[G_0^{R,A}(l\mathbf{k}_2,\omega)]^{N-1}\sum_{\mathbf{p}_1,\mathbf{p}_2,\cdots,\mathbf{p}_a}\Delta(\mathbf{p}_1+\mathbf{p}_2+\cdots+\mathbf{p}_a+\mathbf{k}_1-\mathbf{k}_2)\times\prod_{\alpha=1}^{a}[H_{m_\alpha}(\mathbf{p}_\alpha)H_{n_\alpha}(-\mathbf{p}_\alpha)]\prod_{\mu=a+1}^{a+b}H_{m_\mu}(0)\prod_{\nu=a+1}^{a+c}H_{m_\nu}(0), \tag{3.6}$$

where we define $\mathbf{M}=(m_1,m_2,\ldots,m_a,m_{a+1},\ldots,m_{a+b})$ and $\mathbf{N}=(n_1,n_2,\ldots,n_{a+1},\ldots,n_{a+c})$ under $\sum_{\mu=1}^{a+b}m_\mu=M$ and $\sum_{\nu=1}^{a+c}n_\nu=N$. Here m_μ and n_ν are the numbers of the interaction lines connected with the upper line and the lower line, respectively; m_μ and n_ν for $1\leq\mu\leq a$ belong to the A group, m_μ for $a+1\leq\mu\leq a+b$ to the B group, and n_ν for $a+1\leq\nu\leq a+c$ to the C group. Defining also $u_\mu=G_0^R(l\mathbf{k}_1,\omega)U_i(\mathbf{r}_\mu)$ for $1\leq\mu\leq a+b$, $v_\nu=G_0^R(l\mathbf{k}_2,\omega)U_i(\mathbf{r}'_\nu)$ for $1\leq\nu\leq a$, and $v_\nu=G_0^R(l\mathbf{k}_2,\omega)U_i(\mathbf{r}_\nu)$ for $a+1\leq\nu\leq a+c$, and using the relation

$$\Delta(\mathbf{k})=\frac{1}{V}\int d\mathbf{r}\exp(j\mathbf{k}\cdot\mathbf{r})\ , \tag{3.7}$$

we obtain

$$S(\mathbf{M},\mathbf{N})=\frac{n_i^{a+b+c}}{G_0^R(l\mathbf{k}_1,\omega)G_0^R(l\mathbf{k}_2,\omega)V^a}\times\sum_{\mathbf{p}_1,\mathbf{p}_2,\cdots,\mathbf{p}_a}\int\mathcal{D}\mathbf{r}_a\int\mathcal{D}\mathbf{r}'_a\int\mathcal{D}\mathbf{r}_b\int\mathcal{D}\mathbf{r}_c\prod_{\mu=1}^{a+b}(u_\mu)^{m_\mu}\prod_{\nu=1}^{a+c}(v_\nu)^{m_\nu}\times\frac{1}{V}\int d\mathbf{r}\exp\left[j\sum_{\alpha=1}^{a}\mathbf{k}_\alpha\cdot(\mathbf{r}_\alpha-\mathbf{r}'_\alpha+\mathbf{r})+j(\mathbf{k}_1-\mathbf{k}_2)\cdot\mathbf{r}\right]\ , \tag{3.8}$$

where $\int\mathcal{D}\mathbf{r}'_a=\int d\mathbf{r}'_1\int d\mathbf{r}'_2\cdots\int d\mathbf{r}'_a$ and $\int\mathcal{D}\mathbf{r}_a$, $\int\mathcal{D}\mathbf{r}_b$, and $\int\mathcal{D}\mathbf{r}_c$ are defined in a similar way. With the use of $S(\mathbf{M},\mathbf{N})$ above, the two-particle Green's function is obtained as

$$K^{R,A}(l\mathbf{k}_1,l\mathbf{k}_2;\omega)=G_0^R(l\mathbf{k}_1,\omega)G_0^R(l\mathbf{k}_2,\omega)\sum_{a,b,c}\frac{n_i^{a+b+c}}{a!b!c!}\sum_{\mathbf{M}}{}'P(\mathbf{M};M)\sum_{\mathbf{N}}{}'P(\mathbf{N};N)S(\mathbf{M},\mathbf{N})\ . \tag{3.9}$$

Here $P(\mathbf{M};M)$ is defined as Eq. (2.20) noting the relations for $\mathbf{M}$, $\mathbf{N}$, M, and N given just below Eq. (3.6); $\sum'_M$ means the restricted summation over $m_\mu\geq 1$ $(1\leq\mu\leq a+b)$, and the summation over a, b, and c is over $a\geq 0$, $b\geq 0$, and $c\geq 0$. It is easily seen that we have

$$\sum_{\mathbf{M}}P(\mathbf{M};M)\prod_{\mu=1}^{a+b}(u_\mu)^{m_\mu}=\sum_{m_a+m_b=M}\frac{M!}{M_a!M_b!}\sum_{\mathbf{M}_a}{}'P(\mathbf{M}_a,M_a)\sum_{\mathbf{M}_b}{}'P(\mathbf{M}_b;M_b)\prod_{\mu=1}^{a+b}(u_\mu)^{m_\mu}\ , \tag{3.10}$$

where $\mathbf{M}_a=(m_1,m_2,\ldots,m_a)$ and $\mathbf{M}_b=(m_{a+1},m_{a+2},\ldots,m_{a+b})$ under $\sum_{\mu=1}^{a} m_\mu=M_a$ and $\sum_{\mu=a+1}^{a+b} m_\mu=M_b$. A similar relation is obtained for $P(\mathbf{N};N)$ and v_ν's.

As extensions of Eqs. (2.23) and (2.24), we define

$$Q(u_1,u_2,\ldots,u_k;M_n)=\sum_{\mathbf{M}_k}{}' P(\mathbf{M}_k;M_k)\prod_{\alpha=1}^{k}(u_\alpha)^{m_\alpha}\ , \tag{3.11}$$

$$R(u_1,u_2,\ldots,u_k;M_n)=\sum_{\mathbf{M}_k} P(\mathbf{M}_k;M_k)\prod_{\alpha=1}^{k}(u_\alpha)^{m_\alpha}\ , \tag{3.12}$$

under $k\le n$. Equations (2.23) and (2.24) are related to the above equations as $Q(k;M_n)=\int \mathcal{D}\mathbf{r}_n Q(u_1,u_2,\ldots,u_k;M_n)$ and $R(k;M_n)=\int \mathcal{D}r_n R(u_1,u_2,\ldots,u_k;M_n)$. Note the relation $R(u_1,u_2,\ldots,u_k;M_n)=(u_1+u_2+\cdots+u_k)^{M_n}$ corresponding to Eq. (2.26). As shown in Appendix C, we find the relation

$$Q(u_1,u_2,\ldots,u_k;M_n)=\sum_{\alpha=0}^{k-1}(-1)^\alpha\sum_{(n)}R(u_{n_1},u_{n_2},\ldots,u_{n_{k-\alpha}};M_n)\ , \tag{3.13}$$

corresponding to the relation (2.25). In the equation u_{h_μ} ($\mu=1,2,\ldots,k-\alpha$) agrees with some one of $u_1,u_2,\ldots,u_k$ and $\sum_{(h)}$ means a sum for all possible combinations of $(u_{h_1},u_{h_2},\ldots,u_{h_{k-\alpha}})$ under the restriction that u_{h_μ} with smaller μ should take u_β with smaller β. It should be noted that $Q(u_1,u_2,\ldots,u_n;M_n)$ given by Eq. (3.13) is zero, especially under $1\le M_n<n$. With the use of Eqs. (2.28) and (3.10)–(3.13), we can rewrite Eq. (3.9) as

$$\begin{aligned}K^{R,A}(l\mathbf{k}_1,l\mathbf{k}_2;\omega)&=\mp\sum_{a,b,c}\frac{n_i^{a+b+c}}{a!b!c!}V^{b+c}[h_2^b-(-1)^b][h_3^c-(-1)^c]\int_0^\infty ds\exp\left[\frac{js}{G_0^R(l\mathbf{k}_1,\omega)}\right]\int_0^\infty ds'\exp\left[\frac{\pm js'}{G_0^R(l\mathbf{k}_2,\omega)}\right]\\&\times\frac{1}{V}\int d\mathbf{r}\exp[j(\mathbf{k}_1-\mathbf{k}_2)\cdot\mathbf{r}]\sum_{\alpha=0}^{a-1}(-1)^\alpha\sum_{\beta=0}^{a-1}(-1)^\beta\\&\times\sum_{(g),(h)}\int\mathcal{D}\mathbf{r}_a\left[\exp\left[-j\sum_{\mu=1}^{a-\alpha}U_i(\mathbf{r}_{g_\mu})s\right]-1\right]\int\mathcal{D}\mathbf{r}'_a\left[\exp\left[\mp j\sum_{\nu=1}^{a-\beta}U_i(\mathbf{r}'_{h_\nu})s'\right]-1\right]\\&\times\prod_{\mu=1}^{a}\delta(\mathbf{r}_\mu-\mathbf{r}'_\mu+\mathbf{r})\ ,\end{aligned} \tag{3.14}$$

where $h_2=h(s)$ and $h_3=h(\pm s')$ under the definition (2.30). In these expressions the upper and lower signs of $\pm$ or $\mp$ are chosen according to selective choice of R and A, respectively, of the affix R,A. Equation (3.14) can be rewritten in the form

$$\begin{aligned}K^{R,A}(l\mathbf{k}_1,l\mathbf{k}_2;\omega)=\mp\sum_{a,b,c}\frac{(n_iV)^{a+b+c}}{a!b!c!}[h_2^b-(-1)^b][h_3^c-(-1)^c]\\\times\int ds\exp\left[\frac{js}{G_0^R(l\mathbf{k}_1,\omega)}\right]\int ds'\exp\left[\frac{\pm js'}{G_0^R(l\mathbf{k}_2,\omega)}\right]\\\times\frac{1}{V}\int d\mathbf{r}\exp[j(\mathbf{k}_1-\mathbf{k}_2)\cdot\mathbf{r}][I(\mathbf{r})+(1-h_2)^a+(1-h_3)^a-1]\ ,\end{aligned} \tag{3.15}$$

where

$$I(\mathbf{r})=\sum_{\alpha=0}^{a-1}(-1)^\alpha\sum_{\beta=0}^{a-1}(-1)^\beta J(a-\alpha,a-\beta;\mathbf{r})=\sum_{\alpha=1}^{a}(-1)^{a-\alpha}\sum_{\beta=1}^{a}(-1)^{a-\beta}J(\alpha,\beta;\mathbf{r})\ . \tag{3.16}$$

Here we define

$$J(\alpha,\beta;\mathbf{r})=\sum_{(g),(h)}\int\mathcal{D}\mathbf{r}_a\exp\left[-j\sum_{\mu=1}^{\alpha}U_i(\mathbf{r}_{g_\mu})s\mp j\sum_{\nu=1}^{\beta}U_i(\mathbf{r}_{h_\nu}+\mathbf{r})s'\right]\ . \tag{3.17}$$

Defining

$$h_1=\frac{1}{V}\int d\mathbf{r}'\{\exp[-jU_i(\mathbf{r}')s\mp jU_i(\mathbf{r}'+\mathbf{r})s']-1\}\ , \tag{3.18}$$

we obtain

$$J(\alpha,\beta;\gamma)=\sum_{\mu=0}^{\min(\alpha,\beta)}\frac{a!}{\mu!(\alpha-\mu)!(\beta-\mu)!(a-\alpha-\beta-\mu)!}\ , \tag{3.19}$$

where $\min(\alpha,\beta)$ is equal to the smaller of α and β. From Eqs. (3.16) and (3.19) we obtain

$$\begin{aligned}
&I(\mathbf{r})+(1-h_2)^a+(1-h_3)^a-1\\
&=\sum_{\alpha=0}^{a}\sum_{\beta=0}^{a}\sum_{\mu=0}^{\min(\alpha,\beta)}\frac{a!}{\mu!(\alpha-\mu)!(\beta-\mu)!(a-\alpha-\beta+\mu)!}(h_1+1)^{\alpha}(-h_2-1)^{\alpha-\mu}(-h_3-1)^{\beta-\mu}\\
&=\sum_{m_1=0}^{a}\sum_{m_2=0}^{a}\sum_{m_3=0}^{a}\frac{a!}{m_1!m_2!m_3!(a-m_1-m_2-m_3)!}(h_1+1)^{m_1}(-h_2-1)^{m_2}(-h_3-1)^{m_3}\\
&\quad\times\zeta(a-m_1-m_2)\zeta(a-m_1-m_3)\ ,
\end{aligned} \tag{3.20}$$

where $\zeta(p)=1$ for $p\geq 0$ and $\zeta(p)=0$ for $p<0$. Defining an operator

$$\mathcal{I}(x)=\frac{1}{2\pi j}\int_{-\infty}^{\infty}\frac{dx}{x-j0^+}\ , \tag{3.21}$$

we have

$$\zeta(p)=\mathcal{I}(x)\exp[j(p+0^+)x]\ . \tag{3.22}$$

Using this relation, the term in the last step of Eq. (3.20) is rewritten as

$$\begin{aligned}
&\sum_{m_1=0}^{a}\sum_{m_2=0}^{a}\sum_{m_3=0}^{a}\frac{a!}{m_1!m_2!m_3!(a-m_1-m_2-m_3)!}(h_1+1)^{m_1}(-h_2-1)^{m_2}(-h_3-1)^{m_3}\\
&\qquad\times\mathcal{I}(x_1)\mathcal{I}(x_2)\exp[j(a-m_1-m_2+0^+)x_1+j(a-m_1-m_3+0^+)x_2]\\
&=\mathcal{I}(x_1)\mathcal{I}(x_2)\exp[j(a+0^+)x_1+j(a+0^+)x_2][h_1\exp(-jx_1-jx_2)-h_2\exp(-jx_1)-h_3\exp(-jx_2)+1]^a\ .
\end{aligned} \tag{3.23}$$

Substitution of this term into Eq. (3.15) yields

$$\begin{aligned}
K^{R,A}(l\mathbf{k}_1,l\mathbf{k}_2;\omega)=\mp\int_0^{\infty}ds\exp\left[\frac{js}{G_0^R(l\mathbf{k}_1,\omega)}\right]\\
\times\int_0^{\infty}ds'\exp\left[\frac{\pm js'}{G_0^{R,A}(l\mathbf{k}_2,\omega)}\right]\\
\times[\exp(n_iVh_2)-\exp(-n_iV)][\exp(n_iVh_3)-\exp(-n_iV)]\\
\times\frac{1}{V}\int d\mathbf{r}\exp[j(\mathbf{k}_1-\mathbf{k}_2)\cdot\mathbf{r}]\mathcal{I}(x_1)\mathcal{I}(x_2)\exp[j0^+(x_1+x_2)]\\
\times\exp\{n_iV[h_1-h_2\exp(jx_2)-h_3\exp(jx_3)+\exp(jx_1+jx_2)]\}\ .
\end{aligned} \tag{3.24}$$

Because of $|\mathrm{Re}h_2|\ll 1$ and $|\mathrm{Re}h_3|\ll 1$, we can neglect the term $\exp(-n_iV)$ in the limit $n_iV\to\infty$. Performing the integrations $\mathcal{I}(x_1)$ and $\mathcal{I}(x_2)$, we obtain

$$\begin{aligned}
K^{R,A}(l\mathbf{k}_1,l\mathbf{k}_2;\omega)=\mp\int_0^{\infty}ds\exp\left[\frac{js}{G_0^R(l\mathbf{k}_1,\omega)}\right]\int_0^{\infty}ds'\exp\left[\frac{\pm js'}{G_0^R(l\mathbf{k}_2,\omega)}\right]\\
\times\frac{1}{V}\int d\mathbf{r}\exp[j(\mathbf{k}_1-\mathbf{k}_2)\cdot\mathbf{r}]\exp(n_iVh_1)\ .
\end{aligned} \tag{3.25}$$

As has been done in the preceding section, we take into account the electron-electron interaction by replacing $G_0^R(l\mathbf{k},\omega)$ in the above equation with $G_1^R(l\mathbf{k},\omega)$ given by Eq. (2.31). We obtain a final result

$$K^{R,A}(l\mathbf{k}_1,l\mathbf{k}_2;\omega)=\mp\frac{1}{V}\int d\mathbf{r}\exp[j(\mathbf{k}_1-\mathbf{k}_2)\cdot\mathbf{r}]$$
$$\times\int_0^\infty ds\int_0^\infty ds'\exp\Big[js[\omega-E_l(\mathbf{k}_1)-\Sigma_e^R(l\mathbf{k}_1,\omega)]$$
$$+js'[\omega-E_l(\mathbf{k}_2)-\Sigma_e^R(l\mathbf{k}_2,\omega)]$$
$$+n_i\int d\mathbf{r}'\{\exp[-jU_i(\mathbf{r}')s\mp jU_i(\mathbf{r}'+\mathbf{r})s']-1\}\Big] . \tag{3.26}$$

From this result, the conductivity expressed as Eqs. (3.1) and (3.2) is given by

$$\sigma=\frac{1}{3\pi V}\frac{e^2\hbar^3}{(m^*)^2}\sum_{l,\mathbf{k}_1,\mathbf{k}_2}\mathbf{k}_1\cdot\mathbf{k}_2\int d\omega\frac{d}{d\omega}\Theta(\omega)$$
$$\times\mathrm{Re}[K^R(l\mathbf{k}_1,l\mathbf{k}_2;\omega)$$
$$-K^A(l\mathbf{k}_1,l\mathbf{k}_2;\omega)] . \tag{3.27}$$

It should be noted that this expression convolutes the contributions from the free part and the vertex part shown in Fig. 5.

IV. DISCUSSION FOR PRACTICAL CALCULATION

In this section we put the result obtained in the previous sections in more tractable form. Let us first discuss the screening of the bare potentials starting with the dielectric screening constant $\epsilon(\mathbf{q},\omega)$. Neglecting the retardation effect of the screening, we take $\omega=0$ so that we have

$$\bar{U}_i(\mathbf{q})=\bar{U}_{i0}(\mathbf{q})/\epsilon(\mathbf{q},0) , \tag{4.1}$$

considering the electron-impurity interaction as an example. Noting that $\epsilon(\mathbf{q},0)$ is given in the form

$$\epsilon(\mathbf{q},0)=\epsilon_0(1+\lambda^2/q^2) , \tag{4.2}$$

with the use of the Thomas-Fermi approximation, we obtain

$$U_i(\mathbf{r})=\frac{Ze^2}{\epsilon_0 r}\exp(-\lambda r) . \tag{4.3}$$

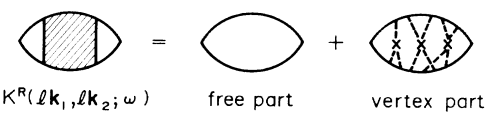

FIG. 5. Diagrams for the free part and the vertex part of the two-particle Green's function $K^R(l\mathbf{k}_1,l\mathbf{k}_2;\omega)$.

In Eq. (4.2), λ is the Thomas-Fermi inverse screening length and ϵ_0 the dielectric constant of the host lattice.

Now we take only the Coulomb term given by Eq. (2.36) as the self-energy for the electron-electron interaction. Defining $\xi=(e^2\lambda/\epsilon_0)s$, $\eta=(e^2\lambda/\epsilon_0)s'$, $\Omega_i=[\omega-E_l(\mathbf{k}_i)]\epsilon_0/(e^2\lambda)$ $(i=1,2)$, $\gamma=4\pi n_i/\lambda^3$, and

$$K^{R,A}(l\mathbf{k}_1,l\mathbf{k}_2;\omega)=-\left[\frac{\epsilon_0}{e^2\lambda}\right]^2\bar{K}^{R,A}(l\mathbf{k}_1,l\mathbf{k}_2;\omega) , \tag{4.4}$$

we obtain

$$\bar{K}^{R,A}(l\mathbf{k}_1,l\mathbf{k}_2;\omega)=\frac{1}{V}\int d\mathbf{r}\exp[j(\mathbf{k}_1-\mathbf{k}_2)\cdot\mathbf{r}]$$
$$\times\bar{G}_{\mathrm{II}}^{R,A}(\Omega_1,\Omega_2;\gamma) . \tag{4.5}$$

Here we define

$$\bar{G}_{\mathrm{II}}^{R,A}(\Omega_1,\Omega_2;\gamma)=\int_0^\infty d\xi\int_0^\infty d\eta\exp[j\xi\Omega_1+j\eta\Omega_2$$
$$+\gamma g_1(\xi,\pm\eta;r)] , \tag{4.6}$$

where

$$g_1(\xi,\pm\eta;r)=\frac{1}{4\pi}\int d\mathbf{y}\left[\exp\left[-\frac{jZ\xi}{y}\exp(-y)\right]\right.$$
$$\left.\mp\frac{jZ\eta}{|\mathbf{y}+\mathbf{x}|}\exp(-|\mathbf{y}+\mathbf{x}|)-1\right]$$
$$+jZ(\xi\pm\eta) \tag{4.7}$$

with $\mathbf{x}=\lambda\mathbf{r}$ $(x=\lambda r)$ and $\mathbf{y}=\lambda\mathbf{r}'$ $(y=\lambda r')$. In Eq. (4.6) we take $+\eta$ for G_{II}^R and $-\eta$ for G_{II}^A. On the other hand, by defining $\Omega=[\omega-E_l(\mathbf{k})]\epsilon_0/(e^2\lambda)$ and

$$G^R(l\mathbf{k},\omega)=\frac{\epsilon_0}{e^2\lambda}\bar{G}^R(\Omega) , \tag{4.8}$$

Eq. (2.32) is rewritten as

$$\bar{G}^R(\Omega)=\frac{1}{j}\int_0^\infty d\xi\exp[j\xi\Omega+\gamma g(\xi)] \tag{4.9}$$

with

$$g(\xi)=\int_0^\infty dy\,y^2\left[\exp\left[-\frac{jZ\xi}{y}\exp(-y)\right]-1\right]+jZ\xi .$$
$$\tag{4.10}$$

An important relation between $g_1(\xi,\pm\eta;r)$ and $g(\xi)$ is that we have

$$\lim_{r\to\infty} g_1(\xi,\pm\eta;r)=g(\xi)+g(\pm\eta)\ . \tag{4.11}$$

Therefore we obtain

$$\lim_{r\to\infty} \bar{G}^{R}_{II}(\Omega_1,\Omega_2;r)=\mp\bar{G}^{R}(\Omega_1)\bar{G}^{R,A}(\Omega_2)\ . \tag{4.12}$$

Now it is noticed that it is impractical to calculate σ from the expression Eq. (3.26) because this expression contains multiple integrations. To facilitate the calculation, we consider the range $r\geq r_c$ where Eq. (4.12) is practically valid; where r_c is some critical value. As a result we obtain

$$\bar{K}^{R,A}(l\mathbf{k}_1,l\mathbf{k}_2;r)=\mp\Delta(\mathbf{k}_1-\mathbf{k}_2)\bar{G}^{R}(\Omega_1)\bar{G}^{R,A}(\Omega_2)$$
$$+\frac{1}{V}\int_{r<r_c} d\mathbf{r}\exp[j(\mathbf{k}_1-\mathbf{k}_2)\cdot\mathbf{r}][G^{R,A}_{II}(\Omega_1,\Omega_2;r)-G^{R,A}_{II}(\Omega_1,\Omega_2;\infty)]\ . \tag{4.13}$$

In obtaining $\Delta(\mathbf{k}_1-\mathbf{k}_2)$ above, we have used Eq. (3.7) with $\mathbf{k}=\mathbf{k}_1-\mathbf{k}_2$. By replacing $\sum_{\mathbf{k}}$ with $[V/(2\pi)^3]\int d\mathbf{k}$, we obtain after some manipulation

$$\sigma=\sigma_1+\sigma_2\ , \tag{4.14}$$

$$\sigma_1=-\frac{1}{3\pi^3}\frac{e^2\hbar^3}{(m^*)^2}\left[\frac{\epsilon_0}{e^2\lambda}\right]^2\sum_l\int d\omega\frac{d}{d\omega}\Theta(\omega)\int_0^\infty dk\,k^4[\mathrm{Im}\bar{G}^{R}(\Omega)]^2\ , \tag{4.15}$$

$$\sigma_2=-\frac{1}{12\pi^4}\frac{e^2}{\hbar}\frac{a_B^2}{\lambda}\sum_l\int d\omega\frac{d}{d\omega}\Theta(\omega)\int_0^{\lambda r_c}dx\int_0^\infty dk_1k_1\int_0^\infty dk_2k_2\left[-y_2^2\cos(y_2x)+y_1^2\cos(y_1x)\right.$$
$$+\frac{2}{x}[y_2\sin(y_2x)-y_1\sin(y_1x)]$$
$$\left.+\left[\frac{2}{x^2}+y_0^2\right][\cos(y_2x)-\cos(y_1x)]\right]$$
$$\times\mathrm{Re}[\bar{G}^{R}_{II}(\Omega_1,\Omega_2;x)+\bar{G}^{A}_{II}(\Omega_1,\Omega_2;x)]\ , \tag{4.16}$$

where a_B is the Bohr radius $\hbar^2\epsilon_0/(m^*e^2)$, $y_1=|\mathbf{k}_1-\mathbf{k}_2|/\lambda$, $y_2=(k_1+k_2)/\lambda$, and $y_0^2=(k_1^2+k_2^2)/\lambda^2$; in place of r in $\bar{G}^{R,A}_{II}(\Omega_1,\Omega_2;r)$ we write $x\ (=\lambda r)$. It can be shown that σ_1 coming from the first term of Eq. (4.13) corresponds to the free part, and σ_2 to the vertex part, of the two-particle Green's function, as shown in Fig. 5.

Let us restrict the discussion hereafter to the case of temperature of 0 K. Although the calculation of σ_1 is straightforward, the expression for σ_2 is still in an impractical form because the integration involved is too multiple to be performed on a standard computer. To further facilitate the calculation we study $G^{R,A}_{II}(\Omega_1,\Omega_2,r)$ given by Eq. (4.6). Let us define new variables $\zeta=\xi+\eta$ and $\beta=\xi-\eta$ where $\zeta>0$ and $-\zeta<\beta<\zeta$. Defining $\phi(\zeta,\beta)=g_1(\xi,\eta;r)$ we obtain

$$\bar{G}^{R}_{II}(\Omega_1,\Omega_2;r)=\int_0^\infty d\zeta\int_0^\zeta d\beta\exp[j\tfrac{1}{2}\zeta(\Omega_1+\Omega_2)+j\tfrac{1}{2}\beta(\Omega_1-\Omega_2)+\gamma\phi(\zeta,\beta)]\ , \tag{4.17}$$

$$\bar{G}^{A}_{II}(\Omega_1,\Omega_2;r)=\int_0^\infty d\zeta\exp[j\tfrac{1}{2}\zeta(\Omega_1-\Omega_2)]\mathrm{Re}\int_0^\zeta d\beta\exp[j\tfrac{1}{2}\beta(\Omega_1+\Omega_2)+\gamma\phi(\beta,\zeta)]\ , \tag{4.18}$$

where we have used the relations $g_1(\xi,-\eta;r)=\phi(\beta,\xi)$, $\phi(\xi,-\beta)=\phi(\zeta,\beta)$, and $\phi(-\beta,\zeta)=\phi^*(\beta,\zeta)$, which are found directly from Eq. (4.7). Integration by parts is performed over β or ζ in each of Eqs. (4.17) and (4.18), respectively, and then use is made of the relation

$$\int_0^\infty d\zeta\int_0^\zeta d\beta\cdots=\int_0^\infty d\beta\int_\beta^\infty d\zeta\cdots$$

followed by interchange of the variables $\beta\rightleftarrows\zeta$. We obtain

$$\mathrm{Re}[\bar{G}^{R}_{II}(\Omega_1,\Omega_2;r)+\bar{G}^{A}(\Omega_1,\Omega_2;r)]=-\frac{2}{\Omega_1-\Omega_2}\mathrm{Re}\int_0^\infty d\zeta\exp[j\tfrac{1}{2}\zeta(\Omega_1+\Omega_2)]$$
$$\times\int_0^\infty d\beta\sin[\tfrac{1}{2}\beta(\Omega_1-\Omega_2)]\frac{\partial}{\partial\beta}\exp[\gamma\phi(\zeta,\beta)]$$
$$=\frac{2}{\Omega_1-\Omega_2}\int_0^\infty d\beta\sin[\tfrac{1}{2}\beta(\Omega_1-\Omega_2)]\frac{\partial}{\partial\beta}\mathrm{Im}\bar{G}^{R}(\tfrac{1}{2}(\Omega_1+\Omega_2),\beta;r)\ . \tag{4.19}$$

The final step is obtained under the definition

$$\bar{G}^{R}(\Omega,\beta;r)=\frac{1}{j}\int_0^{\infty} d\zeta \exp[j\zeta\Omega+\gamma\phi(\zeta,\beta)] . \tag{4.20}$$

As a special case we have $\bar{G}^{R}(\Omega,\beta;0)=\bar{G}^{R}(\Omega,0,0)=\bar{G}^{R}(\Omega)$. For practical calculations it is convenient to use $\mathrm{Im}\bar{G}^{R}(\Omega,\beta;r)=0$ in the range $\Omega>\gamma$, which is shown in Appendix D, because we do not obtain $\mathrm{Im}\bar{G}^{R}(\Omega,\beta;r)=0$ even for $\Omega>\gamma$ in practical calculations, owing to numerical error.

When β is sufficiently large, we have

$$\frac{1}{\Omega_1-\Omega_2}\sin[\tfrac{1}{2}\beta(\Omega_1-\Omega_2)]=\pi\delta(\Omega_1-\Omega_2) . \tag{4.21}$$

Let us define a critical value of β, i.e., β_c, for which the above equation is a good approximation under $\beta\geq\beta_c$. Then we obtain

$$\mathrm{Re}[G_{\mathrm{II}}^{R}(\Omega_1,\Omega_2;r)+G_{\mathrm{II}}^{A}(\Omega_1,\Omega_2;r)]=-2\pi\delta(\Omega_1-\Omega_2)\mathrm{Im}\bar{G}^{R}(\Omega_1,\beta_c;r)$$
$$+\frac{2}{\Omega_1-\Omega_2}\int_0^{\infty} d\beta \sin[\tfrac{1}{2}\beta(\Omega-\Omega_2)]\frac{\partial}{\partial\beta}\bar{G}^{R}(\tfrac{1}{2}(\Omega_1+\Omega_2),\beta;r) . \tag{4.22}$$

If β is sufficiently small, the second term of the above equation is negligible because we then have approximately

$$\frac{\partial}{\partial\beta}\cdots=\left[\frac{\partial\xi}{\partial\beta}\frac{\partial}{\partial\xi}+\frac{\partial\eta}{\partial\beta}\frac{\partial}{\partial\eta}\right]\cdots=\left[\frac{\partial}{\partial\xi}-\frac{\partial}{\partial\eta}\right]\cdots=0 .$$

An actual calculation shows that the contribution of the second term on the right-hand side of Eq. (4.22) to σ is negligible as compared with that of the first term even if β is not so small. Thus the second term in Eq. (4.22) is omitted as an approximation. Final forms of σ_1 and σ_2 for a practical calculation are

$$\sigma_1=\frac{2\sqrt{2}}{3\pi^3}\frac{e^2}{\hbar}\left[\frac{\lambda}{a_B}\right]^{1/2}\sum_l\int_{-\infty}^{\Omega_F} d\Omega(\Omega_F-\Omega)^{3/2}[\mathrm{Im}\bar{G}^{R}(\Omega)]^2 , \tag{4.23}$$

$$\sigma_2=\frac{\lambda}{6\pi^3}\frac{e^2}{\hbar}\int_0^{x_c} dx\int_{-\infty}^{\Omega_F} d\Omega[\mathrm{Im}\bar{G}^{R}(\Omega,\beta_c;x)-\mathrm{Im}\bar{G}^{R}(\Omega,\beta_c;\infty)]$$
$$\times\left\{\frac{2}{x^2}\left[1-\cos\left[\frac{2k}{\lambda}x\right]\right]-\frac{4k}{x\lambda}\sin\left[\frac{2k}{\lambda}x\right]+\frac{2k^2}{\lambda^2}\left[1+\cos\left[\frac{2k}{\lambda}x\right]\right]\right\} , \tag{4.24}$$

where $x_c=\lambda r_c$ and $\Omega_F=[\epsilon_0/(e^2\lambda)]\omega_F$ with ω_F as the Fermi level measured from the band edge; we have $k^2=(2\lambda/a_B)(\Omega_F-\Omega)$.

Now let us discuss the Thomas-Fermi inverse screening length λ. As shown in Appendix E, a general form of λ^2 is given within the framework of the bent-band model as

$$\lambda^2=-\frac{8e^2}{\epsilon_0 V}\sum_{l,\mathbf{k}_1,\mathbf{k}_2}\int d\omega\,\Theta(\omega)\mathrm{Im}[K^{R}(l\mathbf{k}_1,l\mathbf{k}_2;\omega)$$
$$-K^{A}(l\mathbf{k}_1,l\mathbf{k}_2;\omega)] , \tag{4.25}$$

considering the arbitrary temperature in general. Since we know the actual form of $K^{R,A}(l\mathbf{k}_1,l\mathbf{k}_2;\omega)$, we can calculate λ from Eq. (4.25). However, as has been seen in the case of the σ calculation, the computation is impractical due to the multiplicity of the integration. Therefore we only take the first term of Eq. (4.13) approximately, i.e., we take the free part of $k^{R,A}(l\mathbf{k}_1,l\mathbf{k}_2;\omega)$. Then considering the temperature of 0 K, we obtain

$$\lambda^2=\frac{8\sqrt{2}}{\pi^2}\left[\frac{\lambda}{a_B}\right]^{3/2}\frac{1}{\lambda}$$
$$\times\sum_l\int_{-\infty}^{\Omega_F} d\Omega_0\int_{-\infty}^{\Omega_0} d\Omega(\Omega_0-\Omega)^{1/2}$$
$$\times\mathrm{Re}\bar{G}^{R}(\Omega)\mathrm{Im}\bar{G}^{R}(\Omega) . \tag{4.26}$$

The right-hand side of the equation also depends on λ implicitly through $\bar{G}^{R}(\Omega)$ as well as explicitly, so that the above equation should be solved for λ. Although the approximation adopted above is not proved to be useful, it is felt that the approximation is good at least for doping levels above the metal-insulator transition simply because the vertex part is found to be not so important for such doping levels in the calculation of the conductivity.

An alternative method of calculating λ is the direct use of the Thomas-Fermi approximation. We have

$$\lambda^2=\frac{4\pi e^2}{\epsilon_0}\frac{\partial}{\partial\omega_F}n(\omega_F) , \tag{4.27}$$

where the electron concentration $n(\omega_F)$ is given by

$$n(\omega_F)=\int_{-\infty}^{\omega_F} d\omega\,\rho(\omega) \tag{4.28}$$

at 0 K; $\rho(\omega)$ is obtained from Eq. (2.35) as

$$\rho(\omega)=-\frac{\sqrt{2}}{\pi^3}\left[\frac{\epsilon_0}{e^2\lambda}\right]^2\left[\frac{\lambda}{a_B}\right]^{3/2} \times\sum_l\int_{-\infty}^{\Omega_\omega} d\Omega(\Omega_\omega-\Omega)^{1/2}\mathrm{Im}\bar{G}^R(\Omega)\ , \tag{4.29}$$

with $\Omega_\omega=[\epsilon_0/(e^2\lambda)](\omega-\Delta E_l)$; ΔE_l is the energy of the edge of the lth band measured from the Fermi level.

V. RESULTS AND DISCUSSION

In this section, the theory in the previous sections is applied to Ge, Si, and GaAs at 0 K. The calculated results are compared with experimental data available on n-type Ge, p-type Ge, and n-type Si at sufficiently low temperatures. Because Ge and Si are indirect-ban-gap materials having equivalent valleys with anisotropic effective masses, the theory in the previous sections should be modified to take into account this situation.

We assume that the intersubband scattering among the equivalent valleys is negligible for both the electron-impurity and the electron-electron interaction. Thus the summations over the band index appearing in a number of expressions should be replaced with the multiplicative factor ν, which is the number of valleys, i.e., $\sum_l\rightarrow\nu$. For the conduction band, the anisotropic effective mass, which is given by the longitudinal and transverse masses $m_\parallel$ and $m_\perp$, respectively, can be defined in the equation of the energy $E(k)$ as

$$E(\mathbf{k})=\frac{\hbar^2}{2}\left[\frac{1}{m_\perp}(k_x^2+k_y^2)+\frac{1}{m_\parallel}k_z^2\right] \tag{5.1}$$

with $\mathbf{k}=(k_x,k_y,k_z)$. Then we obtain

$$\int d\mathbf{k}f(E(\mathbf{k}))=4\pi\left[\frac{2m_D}{\hbar^2}\right]^{3/2}\int dE\sqrt{E}f(E)\ , \tag{5.2}$$

where $f(E)$ is some function of energy appearing in the expressions for the density of states, the conductivity, and the screening. In Eq. (5.2) m_D is the density-of-states mass, i.e., $m_D=(m_\parallel m_\perp^2)^{1/3}$. As the effective mass appearing in the expression for the conductivity, e.g., Eq. (3.1), we can use the conductivity mass m_C given through $m_C^{-1}=(m_\parallel^{-1}+2m_\perp^{-1})/3$. In practice we use $a_B=\hbar^2\epsilon_0/m_De^2$ in Eqs. (4.23), (4.24), (4.26), and (4.29), and multiply the right-hand sides of Eqs. (4.23) and (4.24) by a factor (m_D/m_C). As for the valence band, the effective mass is not so simply given as for the case of the conduction band and we use the empirical values. Band parameters used for the calculations below are listed in Table I.

Now we find a criterion under which the bent-band model is useful. Let the average distance between the nearest impurities be r_0, which is given through

$$\frac{4\pi}{3}r_0^3n_i=1\ . \tag{5.3}$$

TABLE I. Band parameters. m_0 is the electron mass *in vacuo*.

Material	m_C/m_D	m_D/M_0	ϵ_0	ν
n-type Ge	0.12	0.22	15.4	4
p-type Ge	0.31	0.36	15.4	1
n-type Si	0.26	0.33	11.4	6
p-type Si	0.49	0.53	11.4	1
n-type GaAs	0.067	0.067	1.32	1

Then one criterion may be $\lambda r_0/2\lesssim 1$, which requires that there should be a sufficient number of impurities within a screening range. Using Eq. (5.3) and γ defined just above Eq. (4.4), the above criterion is rewritten as

$$\frac{\lambda r_0}{2}=\left[\frac{3}{8\gamma}\right]^{1/3}\lesssim 1\ . \tag{5.4}$$

Figure 6 shows calculated values of $[3/(8\gamma)]^{1/3}$ for Ge and Si of both types and for n-type GaAs. The values are plotted as functions of the doping level, including the critical level n_c for the metal-insulator transition, which is given by Mott[25] as

$$a_Bn_c^{1/3}=0.25\ . \tag{5.5}$$

To obtain γ, we have calculated λ from Eq. (4.27), although Eq. (4.26) is found to give practically the same value as Eq. (4.27). It should be noted that the value of λ calculated for a sufficiently heavy doping is well approximated by the value for unperturbed states. On the other hand, λ becomes much smaller than the value for unperturbed states, as n_i is decreased down to n_c. It is found that $(3/8\gamma)^{1/3}$ is nearly equal to or smaller than unity, as shown in Fig. 6, over the doping range of practical interest. Thus the criterion (5.4) is nearly satisfied.

Now let us go into the discussion of the conductivity. Figure 7 shows a comparison of the present theory (dashed line) with the previous ones[10] (solid lines) and with experiments[10] (open and solid rectangles) at 4.2 K.

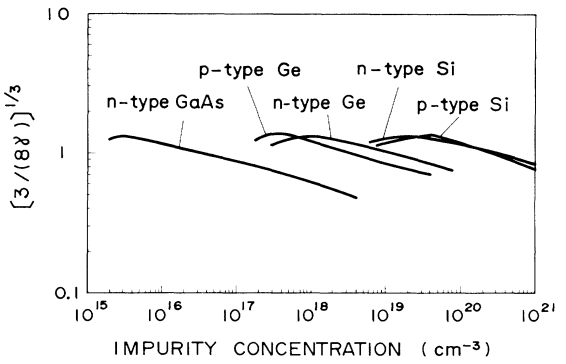

FIG. 6. Number giving a criterion for the validity of the bent-band model, which is shown as a function of the impurity concentration for various materials.

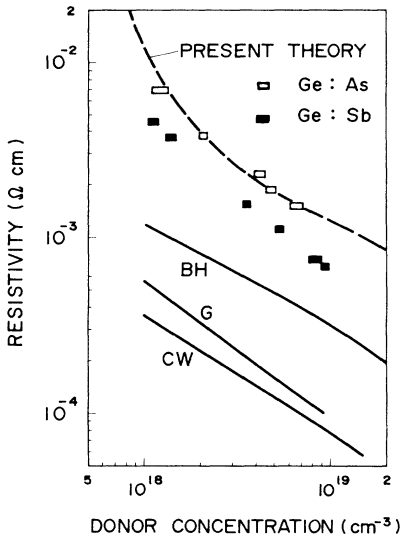

FIG. 7. Resistivity vs the donor concentration, which is obtained from the present theory (dashed line), from previous theories (solid lines) on n-type Ge, and from experiments on Ge:As (solid rectangles), and on Ge:Sb (open rectangles) at 4.2 K.

The solid lines have been calculated by Katz[10] on the basis of the treatments of Conwell-Weisskopf[1] (CW), of Gulyaev[5] (G), and of Brooks-Herring[2] (BH). It is seen that the calculated resistivities of the previous theories are much smaller than the experimental ones on Ge:As (open rectangles) and Ge:Sb (solid rectangles). The main reason of the discrepancy may be that multisite and multiple scatterings are not taken into account in the previous theories. In contrast, the present theory explains experiments very well on Ge:As and considerably well on Ge:Sb.

Figure 8 shows comparisons of the present theory with experiments on n-type Ge and p-type Ge. The solid line and the dashed line are the theoretical results on n-type Ge and p-type Ge, respectively. Experimental data at 4.2 K are shown on Ge:Sb (solid circles[26] and solid rectangles[10]), on Ge:As (open rectangles[10]), and on Ge:Ga (open circles[26]). In the figure the resistivities are plotted versus the net doping level over a wide range covering that around n_c, i.e., $n_c = 9.5\times10^{16}$ cm^{-3} for Ge:Sb,[27] 3.5×10^{17} cm^{-3} for Ge:As,[27] and 1×10^{17} cm^{-3} for Ge:Ga. It is seen that the theory explains the experiments very well on Ge:As and considerably well on Ge:Sb and Ge:Ga at doping levels down to n_c.

Figure 9 shows comparison of the present theory (solid line) with experiments on n-type Si. The experimental data at 4.2 K are shown on Si:P (solid circles[28]) and on Si:As (open circles[29]). The resistivities are plotted versus the net doping level in a wide range covering that around n_c, i.e., $n_c = 3.74\times10^{18}$ cm^{-3} for Si:P (Ref. 29) and 8.5×10^{18} cm^{-3} for Si:As.[29] Agreement between the theory and the experiments is not so bad but is worse than in the case of Ge:As.

There may be two possible causes of the discrepancy between the theory and the experiments. One is the use of the impurity potential of the type given by Eq. (4.3) and the other is the use of the bent-band model. We first discuss the former problem. As is seen in the cases of Ge:Sb and Ge:As and of Si:P and Si:As, experimentally obtained resistivity is different from dopant to dopant of the same type at a given doping level. This may be related with the fact that the impurity binding energy and n_c

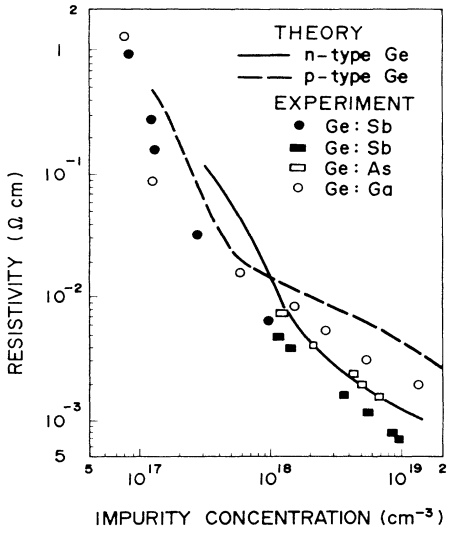

FIG. 8. Resistivity vs the donor or acceptor concentration, which is obtained from the present theory on n-type Ge (solid line) and on p-type Ge (dashed line), and from experiments on Ge:Sb (solid circles and solid rectangles), on Ge:As (open rectangles), and on Ge:Ga (open circles) at 4.2 K.

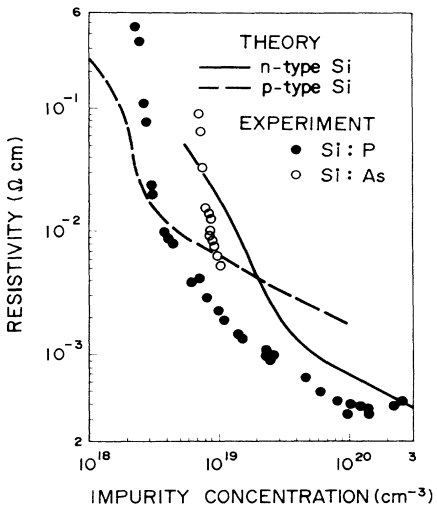

FIG. 9. Resistivity vs the donor or acceptor concentration, which is obtained from the present theory on n-type Si (solid line) and on p-type Si (dashed line), and from experiments on Si:P (solid circles) and on Si:As (open circles) at 4.2 K.

TABLE II. Empirical binding energy and estimated Bohr radius and effective mass. m_0 is the electron mass *in vacuo*.

Material	E_b (meV)	a_B (Å)	m^*/m_0
Ge:As	12.7	36.9	0.22
Ge:Sb	9.7	48	0.17
Ge:Ga	11	43	0.19
Si:P	45.3	14.0	0.43
Si:As	53.5	11.8	0.51

are also different from dopant to dopant. The dopant dependences are considered to arise from the effective impurity potential which is different for different dopants in a region especially near the impurity atom. A convenient method, which is often adopted, of taking into account the effect of the impurity potential is an appropriate choice of the Bohr radius a_B so that the binding energy E_b, given by $E_b = e^2/2a_B\epsilon_0$ in the hydrogenic picture, may agree with an experimental value.[29] In the hydrogenic picture, a_B is given by $a_B = \hbar^2\epsilon_0/m^*e^2$, from which an empirical value of the effective mass m^* can be obtained as an adjustable parameter. In Table II we show experimental values of E_b and the values of a_B and m^* chosen as mentioned just above. By comparing Tables I and II, we find that the values of m^* and m_D show good agreement especially in the case of Ge:As, suggesting that use of Eq. (4.3) as an impurity potential is suitable. This may be the reason why the theory and the experiments of the conductivity show good agreement, especially on Ge:As. We see that m^* and m_D are very different on other materials.

Now we consider another criterion for the bent-band model, which requires that there should be a sufficient number of impurities within one wavelength, i.e.,

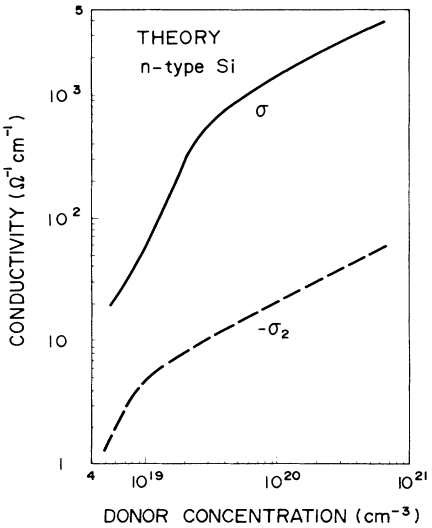

FIG. 10. Conductivities vs the donor concentration, which are obtained from the present theory on n-type Si for σ and σ_2 with $\sigma = \sigma_1 + \sigma_2$.

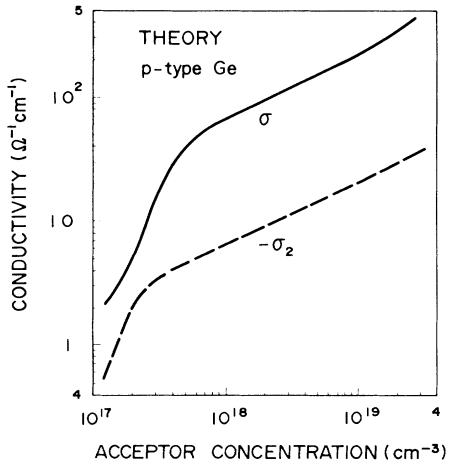

FIG. 11. Conductivities vs the acceptor concentration, which are obtained from the present theory on p-type Ge for σ and σ_2 with $\sigma = \sigma_1 + \sigma_2$.

$$\frac{k}{2\pi} r_0 \lesssim 1 \tag{5.6}$$

for a given wave vector $\mathbf{k}$. For a sufficiently heavy doping, we have $k \leq k_F$, where k_F is the magnitude of the Fermi wave vector given by $k_F = (3\pi^2 n_i/\nu)^{1/3}$, so that we obtain $(k/2\pi)r_0 \leq (k_F/2\pi)r_0 \sim 0.3/\nu^{1/3}$. Therefore the criterion (5.6) is satisfied for a heavy doping. On the other hand, especially when n_i is below n_c, we have nearly bound states so that we have $k/2\pi \lesssim a_B^{-1}$. Especially for $k/2\pi \sim a_B^{-1}$, the criterion (5.6) is rewritten as $a_B n_i^{1/3} \gtrsim (3/4\pi)^{1/3} > 0.25$. In view of Eq. (5.5), therefore, the bent-band model may not be so useful for $n_i \lesssim n_c$. However, for $n_i > n_c$ the bent-band model is considered to be useful, as seen just above, and the discrepancy between the theory and the experiments may be ascribed mainly to inappropriate choice of the impurity potential as given by Eq. (4.3).

Now let us discuss the contribution of the vertex part to

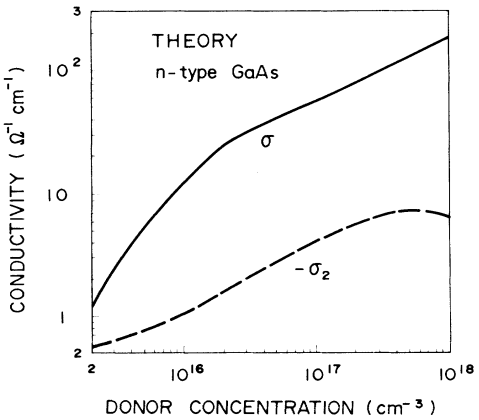

FIG. 12. Conductivities vs the donor concentration, which are obtained from the present theory on n-type GaAs for σ and σ_2 with $\sigma = \sigma_1 + \sigma_2$.

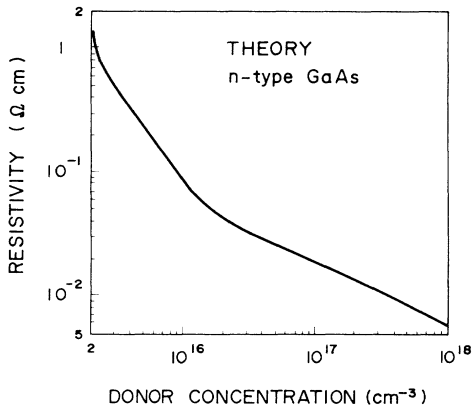

FIG. 13. Resistivity vs the donor concentration, which is obtained from the present theory on n-type GaAs.

the conductivity, which is represented by σ_2 given by Eq. (4.24). It is found that σ_2 is negative and positive for n_i giving $E_F \gtrsim 0$ and $E_F \lesssim 0$, respectively, where E_F is the Fermi level measured from the unperturbed band edge. The value of n_i giving $E_F=0$ may define approximately a theoretical value of n_c. As discussed above, the bent-band model is not useful for $n_i < n_c$ so that positive values of σ_2 obtained may be incorrect. From this viewpoint, in Figs. 6–8 we have shown theoretical σ-n_i curves only in the ranges of n_i where σ_2's are negative.

In Figs. 10–12, we show σ_2's as functions of the doping level for n-type Si, p-type Ge, and n-type GaAs, respectively, as examples. It is seen that the contribution of σ_2 to σ becomes important as n_i is decreased toward n_c. We find that the contribution of σ_2 to σ is very important especially in n-type GaAs. As a result, the conductivity shows a steep rise with decreasing n_i down to n_c in this material, as shown in Fig. 13. It is suggested therefore the σ_2 offers the cause of strong localization as far as it is calculated on some more correct method. Use of the pseudopotential approach to the Green's-function formalism, which has been developed by the present author[30] especially for band-tail states, may be one of such methods where Eq. (4.25) should be used for λ. Use of an appropriate effective impurity potential in combination with the above approach may offer a comprehensive understanding of the quantitative behavior of the conductivity over the whole range of the doping level, although this is beyond the scope of the present work.

ACKNOWLEDGMENTS

The author wishes to express his appreciation to Dr. G. Kano, Dr. I. Teramoto, and Dr. H. Mizuno for their constant encouragement.

APPENDIX A

We prove the validity of the formula

$$Q(k,M_n)=\sum_{\alpha=0}^{k-1}(-1)^{\alpha}\begin{bmatrix}k\\ \alpha\end{bmatrix}R(k-\alpha;M_n) \tag{A1}$$

given in Eq. (2.25) under $k \le n$. From the definition of $Q(k,M_n)$ and $R(k;M_n)$ given by Eqs. (2.23) and (2.24), we directly obtain

$$Q(1;M_n)=\int \mathcal{D}\mathbf{r}_n(u_1)^{M_n}=R(1;M_n)\ , \tag{A2}$$

so that Eq. (A1) holds for $k=1$. It is also easy to see directly

$$Q(2;M_n)=R(2;M_n)-\begin{bmatrix}2\\ 1\end{bmatrix}R(1;M_n)\ , \tag{A3}$$

so that Eq. (A1) holds for $k=2$. Now we assume that Eq. (A1) is valid for $k \le l$ ($<n$). From the definition of $Q(k;M_n)$ and $R(k;M_n)$, we obtain

$$Q(l+1;M_n)=R(l+1;M_n)-\sum_{\alpha=1}^{l}\begin{bmatrix}l+1\\ \alpha\end{bmatrix}Q(l+1-\alpha;M_n)\ . \tag{A4}$$

Because $Q(l+1-\alpha;M_n)$ is given in the form (A1) under $1 \le \alpha \le l$ from the assumption above, Eq. (A4) is rewritten as

$$Q(l+1;M_n)=R(l+1;M_n)-\sum_{\alpha=1}^{l}\begin{bmatrix}l+1\\ \alpha\end{bmatrix}\sum_{\beta=0}^{1-\alpha}(-1)^{\alpha}\begin{bmatrix}l+1-\alpha\\ \beta\end{bmatrix}\times R(l+1-\alpha-\beta;M_n)\ . \tag{A5}$$

This equation can be rewritten in the form

$$Q(l+1;M_n)=\sum_{\beta=0}^{l}A_{\beta}R(l+1-\beta;M_n)\ , \tag{A6}$$

where A_β is determined from Eq. (A5) as

$$A_0=1 \tag{A7}$$

and

$$\begin{aligned}A_{\beta}&=-\sum_{\alpha=1}^{\beta}\begin{bmatrix}l+1\\ \alpha\end{bmatrix}(-1)^{\beta-\alpha}\begin{bmatrix}l+1-\alpha\\ \beta-\alpha\end{bmatrix}\\&=(-1)^{\beta}\begin{bmatrix}l+1\\ \beta\end{bmatrix}\sum_{\alpha=1}^{\beta}(-1)^{\alpha-1}\begin{bmatrix}\beta\\ \alpha\end{bmatrix}\\&=(-1)^{\beta}\begin{bmatrix}l+1\\ \beta\end{bmatrix}\ .\end{aligned} \tag{A8}$$

The last step of Eq. (A8) has been obtained by using

$$\sum_{\alpha=0}^{\beta}(-1)^{\alpha}\begin{bmatrix}\beta\\ \alpha\end{bmatrix}=0\ .$$

From Eqs. (A6)–(A8), it is found that Eq. (A1) is valid for $k=l+1$ as long as it is valid for $k \le l$. Because Eq. (A1) is known to be valid for $k=1$ and 2, the equation is valid also for all k's under $k \le n$.

APPENDIX B

An expression for the conductivity which is based on the two-vector dependent Green's function is given in a tractable form. Starting from Kubo's formula,[31] the dc conductivity tensor $\sigma_{\mu\nu}$ is given by[32]

$$\sigma_{\mu\nu}=-\frac{2j}{\pi V}\frac{e^2\hbar^3}{(m^*)^2}\lim_{\omega\to 0}\frac{\partial}{\partial\omega}\sum_{l,\mathbf{k}_1,\mathbf{k}_2}\int d\omega'\Theta(\omega')G^R(l\mathbf{k}_1,l\mathbf{k}_2;\omega'+\omega)\mathrm{Im}G^R(l\mathbf{k}_2,l\mathbf{k}_1;\omega')\ ; \tag{B1}$$

in this expression the spin multiplicity has been taken into account. The equation is easily rewritten as

$$\sigma_{\mu\nu}=-\frac{2j}{\pi V}\frac{e^2\hbar^3}{(m^*)^2}\sum_{l,\mathbf{k}_1,\mathbf{k}_2}\int d\omega'\Theta(\omega')\left[\mathrm{Im}G^R(l\mathbf{k}_2,l\mathbf{k}_1;\omega')\frac{\partial}{\partial\omega'}G^R(l\mathbf{k}_1,l\mathbf{k}_2;\omega')-\mathrm{Im}G^R(l\mathbf{k}_1,l\mathbf{k}_2;\omega')\frac{\partial}{\partial\omega'}G^A(l\mathbf{k}_2,l\mathbf{k}_1;\omega')\right] . \tag{B2}$$

Using abbreviations $G^R(1)=G^R(l\mathbf{k}_1,l\mathbf{k}_2;\omega)$ and $G^R(2)=G^R(l\mathbf{k}_2,l\mathbf{k}_1;\omega)$, the quantity in the large parentheses of Eq. (B2) becomes

$$\mathrm{Im}G^R(2)\frac{\partial}{\partial\omega'}\mathrm{Re}G^R(1)-\mathrm{Im}G^R(1)\frac{\partial}{\partial\omega'}\mathrm{Re}G^R(2)-j\frac{\partial}{\partial\omega'}[\mathrm{Im}G^R(1)\mathrm{Im}G^R(2)] . \tag{B3}$$

On the first and the second terms of Eq. (B3), we see

$$\sum_{\mathbf{k}_1,\mathbf{k}_2}k_{1\mu}k_{2\mu}\int d\omega'\Theta(\omega')\left[\mathrm{Im}G^R(2)\frac{\partial}{\partial\omega'}\mathrm{Re}G^R(1)-\mathrm{Im}G^R(1)\frac{\partial}{\partial\omega'}\mathrm{Re}G^R(2)\right]=0 \tag{B4}$$

by an interchange $\mathbf{k}_1\rightleftarrows\mathbf{k}_2$ for the second term in the large parentheses. On the second term of Eq. (B3) we have

$$\int d\omega'\Theta(\omega')\frac{\partial}{\partial\omega'}[\mathrm{Im}G^R(1)\mathrm{Im}G^R(2)]=-\int d\omega'\frac{d}{d\omega'}\Theta(\omega')\mathrm{Im}G^R(1)\mathrm{Im}G^R(2) \tag{B5}$$

by performing the integration by parts using $\Theta(\omega')=0$ and $G^R(1)=G^R(2)=0$ under $\omega'\to-\infty$. Considering the cubic symmetry, we can put $k_{1\mu}k_{2\mu}=\mathbf{k}_1\cdot\mathbf{k}_2/3$ in Eq. (B2). We finally obtain

$$\sigma=-\frac{2}{3\pi V}\frac{e^2\hbar^3}{(m^*)^2}\sum_{l,\mathbf{k}_1,\mathbf{k}_2}\mathbf{k}_1\cdot\mathbf{k}_2\int d\omega'\frac{d}{d\omega'}\Theta(\omega')\times\mathrm{Im}G^R(l\mathbf{k}_1,l\mathbf{k}_2;\omega')\times\mathrm{Im}G^R(l\mathbf{k}_2,l\mathbf{k}_1;\omega') , \tag{B6}$$

under $\sigma_{\mu\nu}=\Delta(\mu-\nu)\sigma$.

APPENDIX C

We prove the validity of the formula

$$Q(u_1,u_2,\ldots,u_k;M_n)=\sum_{\alpha=0}^{n-1}(-1)^\alpha\sum_{(h)}R(u_{h_1},u_{h_2},\ldots,u_{h_{k-\alpha}};M_n) \tag{C1}$$

given in Eq. (3.13) under $k\le n$. From the definition of $Q(u_1,u_2,\ldots,u_n;M_n)$ and $R(u_1,u_2,\ldots,u_k;M_n)$ given by Eqs. (3.11) and (3.12), we directly obtain

$$Q(u_1;M_n)=R(u_1;M_n) \tag{C2}$$

so that Eq. (C1) holds for $k=1$. It is also easy to see directly

$$Q(u_1,u_2;M_n)=R(u_1,u_2;M_n)-[R(u_1;M_n)+R(u_2;M_n)] , \tag{C3}$$

so that Eq. (C1) holds also for $k=2$. Now we assume that Eq. (C1) is valid for $k\le l\ (<n)$. From the definition of $Q(u_1,u_2,\ldots,u_k;M_n)$ and $R(u_1,u_2,\ldots,u_k;M_n)$ we obtain

$$Q(u_1,u_2,\ldots,u_k;M_n)=R(u_1,u_2,\ldots,u_l,u_{l+1};M_n)-\sum_{\alpha=1}^{l}\sum_{(k)}Q(u_{k_1},u_{k_2},\ldots,u_{k_{l+1-\alpha}};M_n) , \tag{C4}$$

where u_{k_μ} $(\mu=1,2,\ldots,l+1-\alpha)$ agrees with some one of $(u_1,u_2,\ldots,u_{l+1})$ and $\sum_{(k)}$ means a sum for all possible combinations of $(u_{k_1},u_{k_2},\ldots,u_{k_{l+1-\alpha}})$ under the restriction that u_{k_μ} with smaller μ should take u_β with smaller β. Because $Q(u_{k_1},u_{k_2},\ldots,u_{k_{l+1-\alpha}};M_n)$ is given by Eq. (C1) under $1\le\alpha\le l$ from the assumption above, the second term in Eq. (C4) is rewritten as

$$-\sum_{\alpha=1}^{l}\sum_{(k)}\sum_{\beta=0}^{l-\alpha}(-1)^\beta\sum_{(h)}R(u_{h_1},u_{h_2},\ldots,u_{h_{l+1-\alpha-\beta}};M_n) . \tag{C5}$$

Here u_{h_μ} $(\mu=1,2,\ldots,l+1-\alpha-\beta)$ should agree with some one of $u_{k_1},u_{k_2},\ldots,u_{k_{l+1-\alpha}}$ and $\sum_{(h)}$ means the

sum for all possible combinations of $(u_{h_1},u_{h_2},\ldots,u_{h_{l+1-\alpha-\beta}})$ under the restriction that u_{h_μ} with smaller μ should take u_{k_ν} with smaller ν. $\sum_{(k)}$ coming from Eq. (C4) means the sum of all possible combinations of $u_{k_1},u_{k_2},\ldots,u_{k_{l+1-\alpha}}$. Putting $\gamma=\alpha+\beta$, the expression (C5) is rewritten as

$$-\sum_{\alpha=1}^{l}\sum_{(k)}\sum_{\gamma=\alpha}^{l}(-1)^{\gamma-\alpha}R(u_{h_1},u_{h_2},\ldots,u_{h_{l+1-\gamma}};M_n)\ . \tag{C6}$$

Here $\sum_{(k)}$ and $\sum_{(h)}$ refer to $(u_{k_1},u_{k_2},\ldots,u_{k_{l+1-\alpha}})$ and to $(u_{h_1},u_{h_2},\ldots,u_{h_{l+1-\alpha}})$, respectively. Let us call the former group and the latter group as the u_h group and the u_k group, respectively. Each element of the u_h group is found from the u_k group. The expression (C6) is rewritten as

$$-\sum_{\gamma=1}^{l}\sum_{(h)}\sum_{\alpha=1}^{\gamma}\sum_{(k)}(-1)^{\gamma-\alpha}R(u_{h_1},u_{h_2},\ldots,u_{h_{l+1-\gamma}};M_n)\ . \tag{C7}$$

Let us consider the sum $\sum_{(k)}$, which is equal to the number of all the u_k groups containing a given u_h group. In a given u_k group, the number of all the elements which do not agree with those of a u_h group is given by $l+1-\alpha-(l+1-\gamma)=\gamma-\alpha$. On the other hand, the number of the elements in $(u_1,u_2,\ldots,u_{l+1})$ which do not agree with the elements in a u_h group is $l+1-(l+1-\gamma)=\gamma$. Therefore the number of the u_k groups containing a u_h group is $\gamma C_{\gamma-\alpha}(\equiv\gamma C_\alpha)$, which is just $\sum_{(k)}$. With the use of the relation

$$\begin{aligned}\sum_{\alpha=1}^{\gamma}\sum_{(k)}(-1)^{\gamma-\alpha}&=(-1)^{\alpha}\sum_{\alpha=1}^{\gamma}\begin{bmatrix}\gamma\\ \alpha\end{bmatrix}(-1)^{-\alpha}\\ &=-(-1)^{\gamma}\ ,\end{aligned} \tag{C8}$$

the expression (C7) becomes

$$\sum_{\gamma=1}^{l}(-1)^{\gamma}\sum_{(h)}R(u_{h_1},u_{h_2},\ldots,u_{h_{k+1-\gamma}};M_n)\ . \tag{C9}$$

Substitution of this into Eq. (C3) leads us to the conclusion that Eq. (C1) is valid for $k=l+1$ as long as it is valid for $k\le l$. Because Eq. (C1) is known to be valid for $k=1$ and 2, the equation is valid also for all k's under $k\le n$.

APPENDIX D

We show that we have $\mathrm{Im}\bar{G}^R(\Omega,\beta;r)=0$ in the range $\Omega>\gamma$. For this purpose we use the expression

$$\bar{G}^R(\Omega,\beta;r)=\frac{1}{j}\int_0^\infty d\zeta\exp[j\zeta\Omega+\gamma\phi(\zeta,\beta)] \tag{D1}$$

together with

$$\phi(\zeta,\beta)=g_1\left[\frac{\zeta+\beta}{2},\frac{\zeta-\beta}{2};r\right]\ , \tag{D2}$$

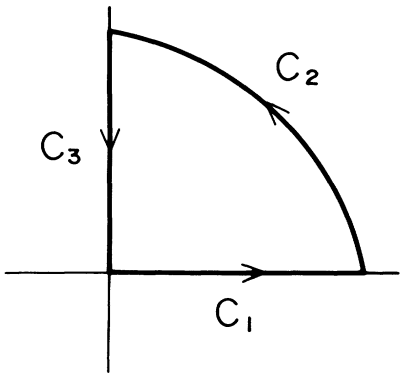

FIG. 14. Paths of the integration over z in the complex plane.

where $g_1(\xi,\eta;r)$ is defined by Eq. (4.7). Consider the integration paths C_1, C_2, and C_3 in the complex plane, as shown in Fig. 14. Because there is no singularity of the integrand of Eq. (D1) in the region enclosed by those paths, the integration path can be transformed from $\int_{C_1}d\zeta\cdots$ in Eq. (D1) to $(\int_{C_2}+\int_{C_3})d\zeta\cdots$. We restrict the discussion to the case of $\bar{Z}<0$ in Eq. (4.7), which is of practical interest in this paper. Then we find that the contour integration over C_2 vanishes only under $\Omega>\gamma$ in the limit of an infinite path radius. As a result we obtain

$$\bar{G}^R(\Omega,\beta;r)=-\frac{1}{j}\int_{j\infty+0}^{j0+0}d\zeta\exp[j\zeta\Omega+\gamma\phi(\zeta,\beta)]\ ,$$

which can be rewritten as

$$\bar{G}^R(\Omega,\beta;r)=\int_0^\infty d\zeta'\exp[-\zeta'\Omega+\gamma\phi(j\zeta',\beta)]\ . \tag{D3}$$

Because $\phi(j\zeta',\beta)$ is found from Eq. (4.7) to be real, we obtain $\mathrm{Im}\bar{G}^R(\Omega,\beta;r)=0$.

APPENDIX E

We derive an expression for the Thomas-Fermi inverse screening length. The expression for the dielectric screening constant is given by[22]

$$\epsilon(\mathbf{q},\omega)=\epsilon_0+V\bar{U}_0(\mathbf{q})M^R(\mathbf{q},\omega)\ , \tag{E1}$$

where $M^R(\mathbf{q},\omega)$ is given by

$$M^R(\mathbf{q},\omega)=\frac{1}{V^2}\sum_{\substack{l,\mathbf{k}_1,\mathbf{k}_2,\\ \sigma_1,\sigma_2}}K_{\mathrm{II}}^R(l\mathbf{k}-\mathbf{q},l\mathbf{k};l\mathbf{k}'+\mathbf{q},l\mathbf{k}';\omega)\ . \tag{E2}$$

Here K_{II}^R is the two-particle retarded Green's function. We first consider the electron-impurity interaction alone. Then we obtain

$$K^R(l\mathbf{k}+\mathbf{q},l\mathbf{k};l\mathbf{k}'-\mathbf{q},l\mathbf{k}';\omega)=\frac{1}{\pi}\int d\omega'\Theta(\omega')[G^R(l\mathbf{k},l\mathbf{k}'+\mathbf{q};\omega'+\omega)\mathrm{Im}G^R(l\mathbf{k}',l\mathbf{k}-\mathbf{q};\omega')$$
$$+G^A(l\mathbf{k}',l\mathbf{k}-\mathbf{q};\omega'-\omega)\mathrm{Im}G^R(l\mathbf{k},l\mathbf{k}'+\mathbf{q};\omega')] \ . \quad \text{(E3)}$$

Now we neglect the retardation effect of the screening and use the Thomas-Fermi approximation. This means that we take $M^R(0,0)$ in Eq. (E1). Then we obtain

$$\epsilon(\mathbf{q},0)=\epsilon_0\left[1+\frac{\lambda^2}{q^2}\right] , \quad \text{(E4)}$$

where λ is a constant given through

$$\lambda^2=\frac{16e^2}{\epsilon_0 V}\sum_{l,\mathbf{k}_1,\mathbf{k}_2}\int d\omega\,\Theta(\omega)\mathrm{Re}G^R(l\mathbf{k}_1,l\mathbf{k}_2;\omega)$$
$$\times\mathrm{Im}G^R(l\mathbf{k}_2,l\mathbf{k}_1;\omega) \ . \quad \text{(E5)}$$

Here the spin multiplicity has been taken into account. Now the ensemble average is taken over the impurity sites, i.e.,

$$\langle \mathrm{Re}G^R(l\mathbf{k}_1,l\mathbf{k}_2;\omega)\mathrm{Im}G^R(l\mathbf{k}_2,l\mathbf{k}_1;\omega)\rangle \ . \quad \text{(E6)}$$

Noting the relation

$$\mathrm{Re}G^R(1)\mathrm{Im}G^R(2)=[G^R(1)G^R(2)-G^R(1)G^A(2)]/2 \ ,$$

where $G^R(i)$ $(i=1,2)$ is the abbreviated expression, we should calculate $\langle G^R(1)G^R(2)\rangle$ and $\langle G^R(1)G^A(2)\rangle$. After taking an ensemble average, we obtain the expression (4.25).

[1]E. Conwell and V. F. Weisskopf, Phys. Rev. **69**, 258 (1946).
[2]H. Brooks, Adv. Electron. Electron Phys. **7**, 85 (1955).
[3]R. B. Dingle, Philos. Mag. **46**, 831 (1955).
[4]P. Csavinsky, Phys. Rev. **126**, 1436 (1962); **131**, 2033 (1963); **135**, AB3 (1964).
[5]Yu V. Gulyaev, Fiz. Tverd. Tela (Leningrad) **1**, 422 (1959) [Sov. Phys.—Solid State **1**, 381 (1959)].
[6]D. Howarth and E. H. Sondheimer, Proc. Phys. Soc. London Sect. A **219**, 53 (1953).
[7]H. Ehrenreich, J. Appl. Phys. **32**, 2155 (1961).
[8]D. L. Rode, in *Semiconductors and Semimetals,* edited by R. K. Willardson and A. C. Beer (Academic, New York, 1975), Vol. 10, Chap. 1.
[9]J. D. Wiley, in Ref. 8, Chap. 2.
[10]M. J. Katz, Phys. Rev. A **140**, 1323 (1965).
[11]T. Matsubara and Y. Toyozawa, Prog. Theor. Phys. **26**, 739 (1961).
[12]V. L. Bonch-Bruevich, in *Semiconductors and Semi-metals,* edited by R. K. Willardson and A. C. Beer (Academic, New York, 1966), Vol. 1 Chap. 4.
[13]M. Takeshima, Phys. Rev. B **25**, 5390 (1982).
[14]M. Takeshima, Phys. Rev. B **33**, 4054 (1986).
[15]M. Takeshima, Phys. Rev. B **34**, 1041 (1986).
[16]M. Takeshima, Phys. Rev. B **33**, 7047 (1986).
[17]M. Takeshima (unpublished).
[18]L. P. Gor'kov, A. I. Larkin, and D. E. Khmelnitzkii, Pis'ma Zh. Eksp. Teor. Fiz. **30**, 248 (1979) [JETP Lett. **30**, 228 (1979)].
[19]D. Volhardt and P. Wölfle, Phys. Rev. B **22**, 4666 (1980).
[20]Y. Ono, J. Phys. Soc. Jpn. **51**, 2055 (1982); **51**, 3544 (1982); **52**, 2492 (1983); **53**, 2342 (1984).
[21]T. Kurosawa and W. Sasaki, J. Phys. Soc. Jpn. **31**, 953 (1971).
[22]A. A. Abrikosov, L. P. Gor'kov, and L. E. Dzyaloshinskii, *Methods of Quantum Field Theory in Statistical Physics* (Prentice-Hall, Englewood Cliffs, 1965).
[23]S. Doniach and E. H. Sondheimer, *Green's Function for Solid State Physicists* (Benjamin, London, 1974).
[24]V. L. Bonch-Bruevich, *The Electronic Theory of Heavily Doped Semiconductors* (Academic, New York, 1966).
[25]N. F. Mott, Can. J. Phys. **34** 1356 (1956).
[26]H. Fritzsche, J. Phys. Chem. Solids **6**, 69 (1958).
[27]M. N. Alexander and D. F. Holcomb, Rev. Mod. Phys. **40**, 815 (1968).
[28]C. Yamanouchi, K. Mizuguchi, and W. Sasaki, J. Phys. Soc. Jpn. **22**, 859 (1967).
[29]P. F. Newman and D. F. Holcomb, Phys. Rev. B **28**, 638 (1983).
[30]M. Takeshima, Phys. Rev. B **30**, 4540 (1984).
[31]R. Kubo, J. Phys. Soc. Jpn. **12**, 570 (1957).
[32]V. L. Bonch-Bruevich, *The Electronic Theory of Heavily Doped Semiconductors* (Academic, New York, 1966).